AD_____

Award Number: W81XWH-06-1-0435

TITLE: Enhancing Quality of Life for Breast Cancer Patients with Bone Metastases

PRINCIPAL INVESTIGATOR: Sarah A. Arrington

CONTRACTING ORGANIZATION: The Research Foundation of SUNY
Syracuse, NY 13210

REPORT DATE: April 2008

TYPE OF REPORT: Annual Summary

PREPARED FOR: U.S. Army Medical Research and Materiel Command
Fort Detrick, Maryland 21702-5012

DISTRIBUTION STATEMENT: Approved for Public Release;
Distribution Unlimited

The views, opinions and/or findings contained in this report are those of the author(s) and should not be construed as an official Department of the Army position, policy or decision unless so designated by other documentation.

REPORT DOCUMENTATION PAGE

1. REPORT DATE	2. REPORT TYPE	3. DATES COVERED
14-04-2008	Annual Summary	15 MAR 2007 - 14 MAR 2008

4. TITLE AND SUBTITLE

Enhancing Quality of Life for Breast Cancer Patients with Bone Metastases

5a. CONTRACT NUMBER

5b. GRANT NUMBER
W81XWH-06-1-0435

5c. PROGRAM ELEMENT NUMBER

6. AUTHOR(S)

Sarah A. Arrington

5d. PROJECT NUMBER

5e. TASK NUMBER

5f. WORK UNIT NUMBER

Email: arringts@upstate.edu

7. PERFORMING ORGANIZATION NAME(S) AND ADDRESS(ES)

The Research Foundation of SUNY
Syracuse, NY 13210

8. PERFORMING ORGANIZATION REPORT NUMBER

9. SPONSORING / MONITORING AGENCY NAME(S) AND ADDRESS(ES)

U.S. Army Medical Research and Materiel Command
Fort Detrick, Maryland 21702-5012

10. SPONSOR/MONITOR'S ACRONYM(S)

11. SPONSOR/MONITOR'S REPORT NUMBER(S)

12. DISTRIBUTION / AVAILABILITY STATEMENT

Approved for Public Release; Distribution Unlimited

13. SUPPLEMENTARY NOTES

14. ABSTRACT   See Next Page.

15. SUBJECT TERMS

 Breast cancer, bone metastasis, animal model, radiation therapy, anabolic agents, bisphosphonates, biomechanical testing, histology

16. SECURITY CLASSIFICATION OF:			17. LIMITATION OF ABSTRACT	18. NUMBER OF PAGES	19a. NAME OF RESPONSIBLE PERSON USAMRMC
a. REPORT	**b. ABSTRACT**	**c. THIS PAGE**	UU	47	**19b. TELEPHONE NUMBER** *(include area code)*
U	U	U			

14. ABSTRACT

Current treatment for osteolytic breast cancer bone metastasis typically involves radiation therapy (RTX) to palliate bone pain and a bisphosphonate to inhibit osteoclastic bone resorption. The goal of this research was to determine the effects of zoledronic acid as an adjunct to RTX on restoring bone strength and density. We also investigated whether the combination of ZA and an anabolic agent (parathyroid hormone, PTH) as adjuncts to RTX further enhanced bone strength and thus decrease the risk of subsequent pathological fractures.

Using our mouse model of breast cancer bone metastasis, we were able to demonstrate that adjunct treatment of a high dose of ZA (600 ug/kg, accumulative dose) alone or in combination with PTH (800 ug/kg, accumulative dose) was capable of restoring bone mineral density (BMD) and mechanical strength to that of a normal bone. This was a significant improvement compared to treatment with RTX alone in which BMD was 36.6% lower compare to normal (p<0.0001) and mechanical strength was 2.4-fold lower compared to normal (p<0.0001). There were no significant differences in BMD or mechanical strength between mice treatment with RTX and ZA or ZA/PTG. In a second series of experiments we were able to demonstrate that a clinically relevant of ZA (100 ug/kg, accumulative dose) as an adjunct to RTX, not only significantly increased BMD compared to treatment with RTX alone (p=0/026), but also significantly increased BMD by 12.7% compared to normal (p=0.049. Based on the results we have seen so far, we have decided that it is not necessary to combine ZA and PTH in order to restore the strength and bone properties of tumor-burdened bone to that of a normal bone. These results have also led us to investigate the effects of ZA on breast cancer cells and osteoblasts in-vitro.

Table of Contents

1. Introduction

The skeleton is the third most common site of metastasis for women with advanced stage breast cancer (26, 34, 82). Severe osteolysis, which commonly occurs during this stage of the disease, can lead to skeletal complications including pathological fracture and severe bone pain. Currently patients are treated with radiation therapy to palliate bone pain and a bisphosphonate to inhibit ongoing osteoclastic bone resorption. Results from clinical trials indicate that anywhere from 6 to 26% of metastatic bone lesions treated with radiation therapy will go on to develop pathological fractures (47, 83). Clinical data has also shown that zoledronic acid, a third generation bisphosphonate, decreased the number of skeletal related events by 39% compared to placebo (49). Clinicians recognize that prevention of skeletal complications considerably improves the quality of life for these patients (23); and although bisphosphonates can decrease the chances of a patient developing a skeletal complication many are still at risk. In an effort to address this issue we hypothesized that the combination of an anabolic agent, parathyroid hormone (PTH 1-34) in conjunction with a bisphosphonate (zoledronic acid, ZA) and radiation therapy (RTX) for the treatment of metastatic bone lesion from breast cancer would stimulate new bone formation, improve mechanical properties, and thus decrease the risk of subsequent pathological fractures.

2. Body

2.1: *Task 1: Evaluation of PTH and ZA as adjuncts to RTX for the treatment of focal breast cancer bone metastasis in the mouse.*

In order to study the effects of PTH and ZA as adjuncts to RTX for the treatment of an established osteolytic bone metastasis from breast cancer, we have utilized a murine model developed in our lab (2), Appendix A. To date, two full studies have been completed and a third study is currently underway (Table 1). Below is a brief description of the materials and methods used for these three studies, followed by results and justifications for the next study. The number of mice used for histology (H), for mechanics (M), and micro-CT (µCT) is included in the table.

Table 1: Experimental Design for *In Vivo* Studies

Mouse Studies			
	Study 1	**Study 2**	**Study 3 (pilot)**
# of tumor cells injected (F10)	1×10^5	2×10^4	1×10^5
Duration	9 Weeks	12 Weeks	Variable
Therapies			
Week initiated post-surgery	3 weeks	4 Weeks	Based on lesion
Drug Dose: All injections were given subcutaneous	ZA: 100µg/kg, weekly for 6 wks PTH: 80µg/kg, daily for 4 wks	ZA: 12.5µg/kg, weekly for 8 wks Or ZA: 25µg/kg weekly for 4 wks, followed by PTH (80µg/kg) daily for 4 wks	ZA: 25µg/kg, weekly for 4 wks Or Saline (vehicle)
0 Gy	H: n = 0 M: n = 6	H: n = 6 M: n = 8	µCT: n = 10
20 Gy	H: n = 6 M: n = 6	H: n = 6 M: n = 8	
20 Gy + ZA	H: n = 6 M: n = 6	H: n =6 M: n = 8	
20 Gy + PTH	H: n = 6 M: n =6		
20 Gy + ZA + PTH	H: n = 6 M: n = 6	H: n = 6 M: n = 8	
ZA	H: n = 6 M: n =6		µCT: n = 10
Status	Accepted for publication November 2007	Preparing manuscript for publication	Pilot study complete

Materials and Methods:
Tumor Cells
F10 cells, a bone-adapted clone derived from the human MDA-MB-231 breast carcinoma cell line (93)(Dr. Toshiyuki Yoneda, UT San Antonio, TX) were used for this study. Cells were cultured in Dulbecco's modification of Eagle's medium (DMEM) supplemented with 10% (v/v) fetal calf serum (FCS) and 1% penicillin-streptomycin-glutamine (Gibco, Grand Island, NY) and maintained at 37ºC in an atmosphere of 5% CO_2 in air.

Tumor Cell Inoculation
Female NCr homozygous nude mice (8 to 9 weeks old, 20-25 grams body weight) (Charles River, Wilmington, MA) were anesthetized with an injectable drug cocktail consisting of telazol (45 mg/kg, IM) and xylazine (7.5 mg/kg, IM). The mice were weighed and the hind limbs scrubbed with betadine followed by 70% ethanol. With the knee flexed, a small incision was made at the joint and the patella carefully moved to expose the distal end of the femur. Using a sterile 26G needle, twenty microliters of cell suspension (containing 1 x 10^5 or 2 x 10^4 F10 breast cancer cells) were injected through the intercondylar fossa of the right femur to a depth of approximately 5 mm. Mice were housed in micro-isolators with a 12-hour day/night cycle and were fed a diet of autoclaved food and water *ad libitum*.

Bone Densitometry
Dual-energy X-ray absorptiometry (DEXA) measurements of the left and right femora were obtained immediately following tumor inoculation and at three, six, nine, and twelve weeks using a dedicated mouse bone densitometer (PIXImus 2; GE Lunar; Madison, WI). Bone mineral density (BMD) values (g/cm^2) were determined from a region of interest that encompassed the entire femur.

Mechanical Testing
Whole-limb torsional testing was performed in order to asses the mechanical strength of tumor burdened bones in which the primary site of osteolysis was in the distal femur. This method has been previously described (2). Briefly, the proximal femur and the distal tibia were embedded in poly-methylmethacrylate (PMMA) using an alignment fixture. The bone was then placed in a torsion testing jig and loaded in external rotation at a rate of 180°/min. The resulting torque (N-mm) was measured. Energy to failure (N-mm-degree) was determined by calculating the area under the torque-rotation curve. Initial stiffness (N-mm/degree) was defined as the first 50% of the slope to torque at failure.

Histological Confirmation of Tumor
Limbs that were selected for histology were embedded in methylmethacrylate (MMA) according to the method described by Erben (27). Embedded bones were then trimmed on a low-speed diamond saw (Buehler, Lake Bluff, IL) and 5-µm sections were cut using a microtome. Sections were stained with modified Masson's trichrome stain and examined by light microscopy to confirm the presence of tumor.

Total Bone Analysis
Prior to sectioning, embedded femora were scanned using a micro-CT scanner (SCANCO µCT 40, SCANCOMedical, Zürich, Switzerland). X-ray acquisition settings were 55 kVp and 145 µA with an integration time of 200-ms. Scans were performed with an isotropic voxel size of 12 µm and images were reconstructed in 1024 x 1024 pixel matrices. A global threshold of 35% maximal grayscale was determined by visual inspection to best distinguish between bone and non-bone material. Measurements of total bone volume in the distal 5 mm of the femur (BV_{tot}) were obtained from transverse slices in which the region of interest (ROI) included both cortical and trabecular bone. For measurements of fractional trabecular bone (BV/TV), the distal femur was reconstructed in the sagital plane. The trabecular bone ROI was drawn to include all cancellous bone in the metaphysis region extending 1 mm from the base of the growth plate.

Statistics
Analysis of variance along with Fisher's PLSD post-hoc was performed to analyze differences between groups. Statistical significance was taken at *P* < 0.05.

Study 1: Response of High Dose ZA with and without anabolic agent (PTH)
The specific aim of this first study was to determine if bone that had been affected by both tumor-induced osteolysis and radiation was capable of regaining normal bone density, mechanical strength and bone morphology. Based on preliminary data, a study period of nine weeks was thought to be sufficient time to see significant improvement in bone density and mechanical strength in tumor-burdened bones treated with ZA, PTH, or ZA/PTH as adjuncts to radiation. Previous work with this model has shown that mice that do not receive treatment rarely survive to nine weeks; therefore, for this study we chose not to have an untreated, 0 Gy group for histology. Since the focus of this study was to determine if diseased bone was capable of "repair", we selected a dose of ZA that was much higher than the dose given clinically. The rationale behind this was due to the fact that this model system produces significant osteolysis that progresses rapidly. Therefore, it was thought that a higher dose of ZA may be required to combat this fast paced bone destruction. In this first study the ZA and PTH were administered concurrently. There is conflicting data in the literature as to whether patients who have been on bisphosphonates and then switch to PTH for treatment of osteoporosis experience a blunted anabolic affect from the PTH (18, 22, 35, 62, 63, 94). Based on this information it was rationalized that giving the two drugs concurrently may provide the best environment for bone "repair". In this first study we also wanted to determine if PTH was capable of restoring bone density and mechanical strength when used in combination with RTX only. Although the use of PTH in patients with cancer is not clinically applicable, it was used in this study to specifically address whether an anabolic agent was capable of "repairing" bone that was affected by both tumor and radiation. The goals of study one were to establish if tumor-burdened bone treated with radiation was capable of being restored to normal in terms of both bone density and mechanical strength; and whether this "repair" could be accomplished with an anti-resorptive agent, such as ZA, an anabolic agent, such as PTH, or if it would require the combined features of an anti-resorptive and an anabolic agent. The results of this study were described in the annual report for 2006 and were subsequently published (**Arrington, JSO 2007**) **(Appendix A).**

Study 2: Response of Clinical Doses of ZA with and without Anabolic Agent (PTH)
The specific aim of this second study was evaluate the effectiveness of a clinically relevant dose of ZA as an adjunct to RTX, with regards to restoring BMD and mechanical properties to that of a normal, non-tumor bearing bone. Based on the results of the first study we wanted to see if the anabolic effects of PTH were affected by administering it after the mouse had been treated with ZA for four weeks. Taking into consideration that the mineralization process requires time to develop, we decided to extend the study period from nine weeks to twelve weeks. This lengthened study time also allows us to evaluate the safety aspects of these drugs in terms of secondary tumor growth in distant organs. In addition to the outcome measures analyzed in the first study, the second study included a more detailed analysis of bone microarchitecture using a microCT scanner that was acquired after the conclusion of the first study. These data allowed us to evaluate the effects of these adjunct therapies on bone geometry and possibly correlate features of the microarchitecture with mechanical strength.

Summary of Key Results:
Survival and Tumor Engraftment
At the end of the study three mice did not show evidence of successful tumor engraftment based on X-ray (two 0Gy and one 20Gy mouse) and were therefore not analyzed. Two mice died during their two-week X-rays due to anesthesia and a third mouse was euthanized at four weeks due to fracture caused by severe osteolysis. Six femora fractured due to very low strength during processing for biomechanical testing and therefore could not be mechanically tested.

Effects of Radiation Therapy on Tumor-Induced Osteolysis: total bone analysis
Progression of tumor-induced osteolysis was assessed using serial radiographs. Osteolysis progressed quickly in mice treated with 0 Gy (Figure 1.1a-b) and none of the mice survived past eight weeks post-tumor injection. Treatment with 20 Gy appeared to slow the progression of osteolysis (Figure 1.1c-e), however significant bone loss was still observed at the end of study (Figure 2.1e). Terminal DEXA and µCT scans confirmed that treatment with 20 Gy significantly increased BMD and total bone volume in the femur compared to treatment with 0 Gy (11.2%, p=0.030 and 47.2%, p=0.032, respectively) (Figure 1.2). A similar trend was seen for measurements of bone mineral mass (Figure 1.2).
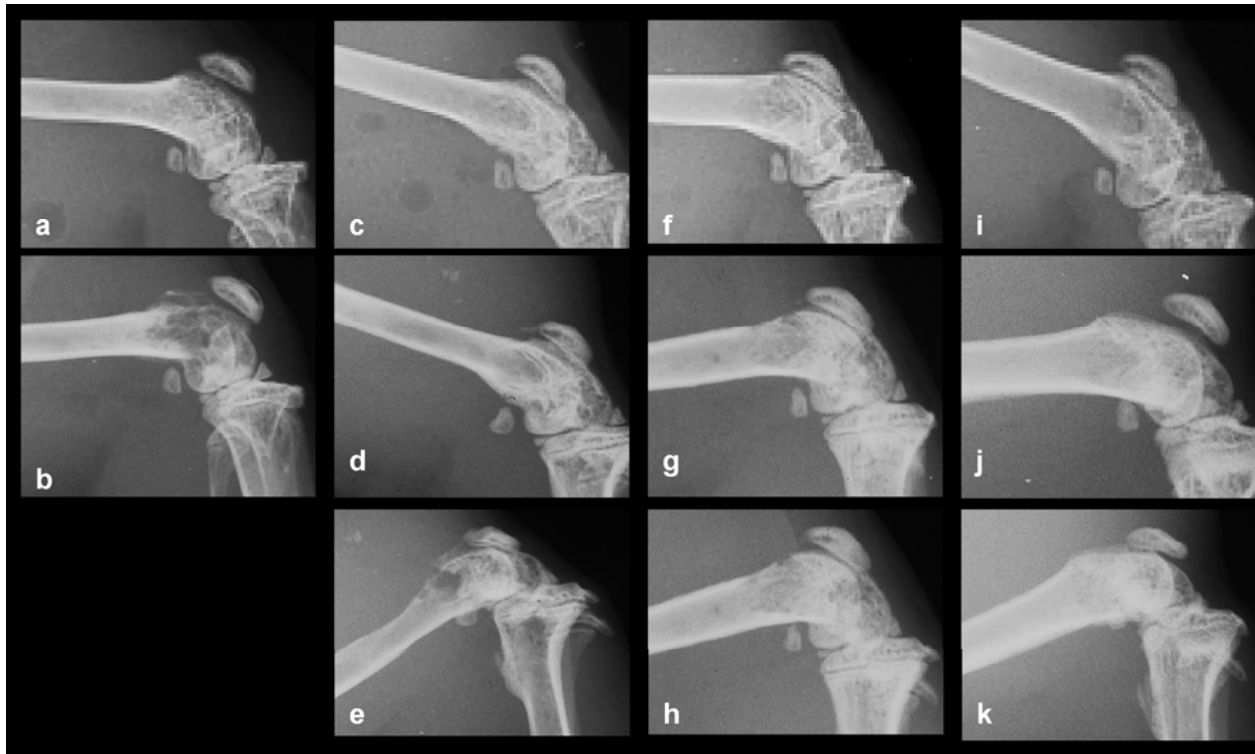
Figure 2.1(a-k): Comparative Radiographs of Femora Demonstrating the Progression of Osteolysis in Tumor-Bearing Bones
Top panel: 4 week radiographs taken at the time of treatment 0Gy (a), 20Gy (c), 20Gy+ZA (f), 20Gy+ZA+PTH (i). Middle panel: 0Gy at 6 weeks (terminal X-ray) (b), 20Gy at 9 weeks (d), 20Gy+ZA at 9 weeks (g), 20Gy+ZA+PTH at 9 weeks (j). Bottom panel (terminal X-rays): 20Gy at 11 weeks (e), 20Gy+ZA at 11 weeks (h), and 20Gy +ZA+PTH at 11 weeks (k). Note the presence of osteolysis in the 0Gy and 20Gy treatment groups.

A

Terminal BMD Relative to Baseline

Figure 2.2(A-C): Quantification of Bone in Tumor-Bearing Femora Compared to Normal.
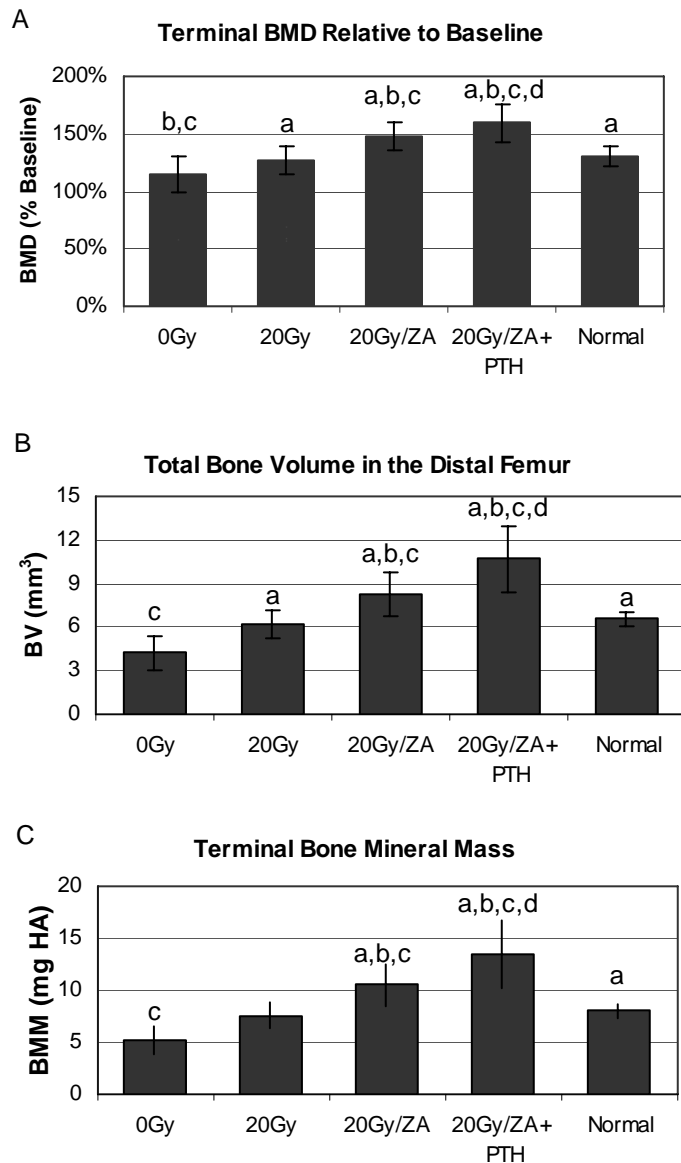BMD measured in the entire femur. Total bone volume (BV_{tot}) in the distal 5 mm (A). Bone mineral mass calculated in the distal 5 mm (B). Terminal bone mineral mass (BMM) in the distal 5 mm (C).
a = significantly different from 0Gy
b = significantly different from 20Gy
c = significantly different from normal
d = 20Gy + ZA + PTH is significantly different from 20Gy + ZA.
Statistical significance was taken at p<0.05)

B

Total Bone Volume in the Distal Femur

C

Terminal Bone Mineral Mass

Effects of Radiation Therapy on Tumor-Induced Osteolysis: microarchitecture and biomechanical strength

Normal bones have an average BV/TV of 17%. Mice treated with 0 Gy sustained a severe loss of trabecular bone with an average BV/TV of less than 1% and mice treated with 20 Gy displayed an average BV/TV of 3% (p=0.025 and p=0.053, respectively compared to normal). There was not a significant difference in trabecular number or thickness between tumor-bearing bones treated with 20 Gy and normal bones (p=0.885 and p=0.798, respectively) (Table 2.2). However, connectivity density was dramatically decreased in the 20Gy treatment group compared to normal (p=0.0007). 3D reconstructions clearly demonstrated substantial trabecular bone loss in bones treated with 20 Gy compared to normal (Figure 1.3). Mice in the 0Gy group did not contain enough trabecular bone for accurate measurements to be made. Consistent with the loss of trabecular bone, tumor-burdened bones treated with 20 Gy exhibited a 46% decrease in peak torque (p=0.045), a 59% decrease in energy to failure (p=0.005), and a 14% decrease in initial stiffness (p=0.726) compared to normal bone (Table 1.3). There was no significant difference in biomechanical strength between the 0Gy and 20Gy treatment groups.

Effect of ZA as an Adjunct to Radiation Therapy

Radiographs clearly demonstrated that 20Gy+ZA reduced the extent of osteolysis compared to 20Gy alone (Figure 1.1c-h). The combination of radiation and ZA increased BMD (p=0.0002), total bone volume (p=0.018), and bone mineral mass (p=0.015) in the tumor-burdened femur compared to 20Gy alone (Figure 1.2). It should be noted that treatment with 20Gy+ZA significantly increased BMD, total bone volume and bone mineral mass in tumor-bearing bones compared to normal (p=0.002, p=0.044, and p=0.039, respectively).

Adjunct treatment with ZA appeared to improve both microarchitecture and biomechanical strength compared to treatment with radiation alone. Mice treated with 20Gy+ZA exhibited very similar fractional trabecular bone volume and microarchitecture to normal bone (Table 2.2). There was no significant difference in BV/TV, trabecular number, trabecular thickness, or connectivity density. Treatment with 20Gy+ZA dramatically improved BV/TV and the microarchitecture of trabecular bone in tumor-burdened bones compared to 20Gy (Figure 1.3 B-C), however the trabecular bone was not completely restored to that of normal bone (Figure 1.3A). Treatment with 20Gy+ZA increased torque at failure 104% (p=0.014) and energy to failure 120% (p=0.015) compared to treatment with 20 Gy alone. There was no significant difference in biomechanical strength between normal bones and tumor-burdened bones treated with 20Gy+ZA (Table 1.3).
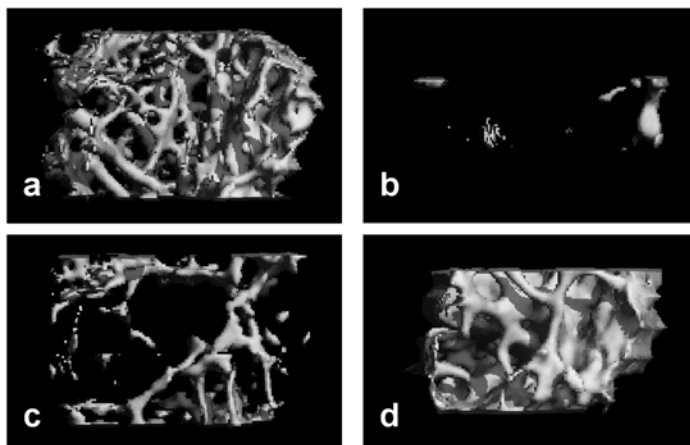

Figure 2.3(a-d): Terminal 3D Micro-CT Reconstructions of Trabecular Bone in Normal and Tumor-Bearing Femora Note the amount of trabecular bone loss observed in femora treated with 20 Gy (b) compared to the bones treated with 20Gy + ZA (c) or 20Gy + ZA + PTH (d). Also note the increased trabecular thickness in bones treated with 20Gy + ZA + PTH (d) compared with normal (a).

Table 2.2: Microarchitecture comparisons between normal bones and tumor-bearing bones treated with 20 Gy, 20Gy + ZA and 20Gy + ZA + PTH (1-34)

Trabecular indices were not calculated for mice treated with 0Gy since BV/TV was less than 1%.

	Normal* (n=5)		20Gy (n=5)			20Gy + ZA (n=6)			20Gy + ZA + PTH (n=4)		
	Mean	SD	Mean	SD	ANOVA *p* Value	Mean	SD	ANOVA *p* Value	Mean	SD	ANOVA *p* Value
BV (mm^3)	6.537	0.476	6.181	0.963	0.683	8.304	1.503	**0.0442**	10.701	2.276	**0.0002**
BV/TV (%)	0.174	0.027	0.029	0.020	0.053	0.175	0.131	0.990	0.217	0.229	0.566
Tb.N. (1/mm)	3.178	0.715	3.383	0.530	0.885	4.471	4.621	0.346	3.882	1.303	0.640
Tb.Th. (mm)	0.064	0.007	0.069	0.015	0.798	0.078	0.021	0.479	0.12	0.068	**0.020**
Con.D. (1/mm^3)	123.2	24.400	5.38	4.920	**0.0007**	75.8	77.800	0.107	103	58.700	0.524

* Normal bones are the left, non-operated limbs of the 20Gy mice; *p*-values are taken with respect to normal

Table 2.3: Effects of ZA and PTH on the mechanical strength of tumor-burdened bone

Treatments	Torque at Failure			Energy to Failure			Initial Stiffness		
	N-mm		ANOVA *P* Value*	N-mm-degree		ANOVA *P* Value*	N-mm/degree		ANOVA *P* Value*
	Mean	SD		Mean	SD		Mean	SD	
Normal (n=7)	16.914	4.316	-	599.12	79.69	-	0.184	0.133	-
0 Gy (n=5)	5.572	6.274	**0.007**	154.53	174.83	**0.001**	0.072	0.092	0.143
20 Gy (n=6)	9.098	5.576	**0.045**	244.98	169.7	**0.005**	0.159	0.102	0.726
20Gy/ZA (n=8)	18.545	9.407	0.640	539.18	329.9	0.584	0.275	0.162	0.176
20Gy/ZA/PTH (n=6)	15.122	5.59	0.633	429.1	150.2	0.155	0.256	0.108	0.312

* *P* Values are with respect to the normal limbs (the left limbs of the 20 Gy mice). Significance taken at *P* < 0.05.

Effect of ZA and PTH as Adjuncts to Radiation Therapy

Similar to the effect seen with 20Gy+ZA, mice treated with 20Gy+ZA+PTH demonstrated decreased osteolysis on X-ray compared to those treated with 20Gy alone (Figure 1.1i-k). There was a marked increase in BMD, total bone volume and bone mineral mass for the 20Gy+ZA+PTH treated mice compared to 20Gy, 20Gy+ZA and normal groups (Figure 1.2). Microarchitecture measures for the 20Gy+ZA+PTH group had higher specimen-to-specimen variability when compared to normal bone, which reduced statistical power (Table 2.2). Average BV/TV increased from 17% measured in normal bones and 20Gy+ZA treated bones, to 22% in the 20Gy+ZA+PTH group (p=0.566 and p=0.559, respectively). Trabecular thickness increased by 54% compared to 20Gy+ZA (p=0.065) and 87% compared to normal (p=0.020). This increase in trabecular thickness is clearly evident on 3D reconstructions of the trabecular bone (Figure 1.3). Tumor-burdened bones treated with 20Gy+ZA+PTH had biomechanical strength measures that were similar to the 20Gy+ZA and normal groups (Table 1.3).

Effect of ZA and PTH on Normal Bone

Unlike radiation therapy which is locally administered to tumor-burdened bones, ZA and PTH are systemic and may have an effect on normal bones. The left, non-tumor bearing femora of the 20Gy+ZA, 20Gy+ZA+PTH treated mice were compared to the left femora of the 20Gy only treated animals (control femora). There was no significant difference in BMD between any of the groups. However, total bone volume in the distal 5 mm was significantly affected by ZA and ZA+PTH. Normal bones exposed to ZA displayed a 42% in BV, where bones exposed to ZA+PTH had a 57% increase in BV compared to normal (p=0.0008 and p=0.0004, respectively) (Figure 1.4). There was no significant difference in total bone volume between the ZA and ZA+PTH treated bones (p=0.245). These results suggest that ZA and ZA+PTH are capable of increasing bone volume in normal, non-diseased bones.
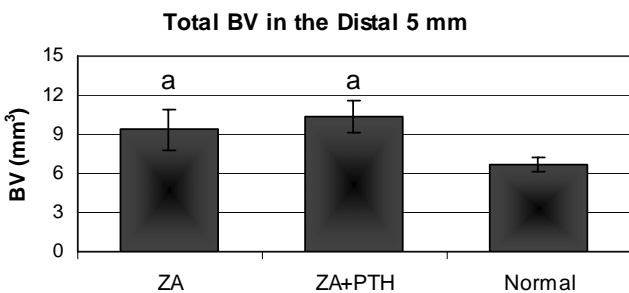

Figure 1.4: Total Bone Volume in the Distal 5 mm of Normal Bone
Non-tumor bearing bones exposed to PTH and/or ZA displayed increased bone volume in the distal 5 mm of the femur compared to normal bone.
a = significantly different from normal.
Significance taken at p<0.05.

DISCUSSION

The model system used in this study allowed us to directly compare the effectiveness of three different therapy regimens with regards to the quality (trabecular microarchitecture) and quantity (BMD and bone volume) of bone and biomechanical strength. There was a large decrease in biomechanical strength in tumor-burdened bones treated only with radiation (20Gy) and this was associated with a decrease in trabecular bone in the distal femur. Interestingly, other measures of bone mass including BMD, total bone volume, and bone mineral mass did not change between the normal and 20Gy treated mice. This suggests that loss of trabecular bone may play an important role in bone strength. A clinically relevant dose of zoledronic acid, given as an adjunct to radiation therapy, improved trabecular micro-architecture, with resulting biomechanical strength not different from normal. In addition, there was accrual of bone such that ZA treated bones had greater total bone volume when compared to normal femora. Finally, the combined adjunct therapy of zoledronic acid (an antiresorptive agent), followed by hPTH(1-34)NH$_2$ (an anabolic agent) did not lead to further increases in bone strength. However, this combined therapy did cause increased trabecular thickness and total bone volume, suggesting that ZA did not blunt the anabolic effect of PTH.

9

Although this pre-clinical *in-vivo* model does not allow us to study the physiological process of bone metastases, including natural spread from a primary tumor, the controlled location allows us to implement consistent radiation therapy and biomechanically test all bones. In addition, the use of immunocompromised mice precludes studies on the immune response. One challenge with the current model system is that tumor osteolysis does not progress at the same rate in all animals. The range of disease progression at the start of treatment may also impact the effectiveness of the therapies. Interestingly, in this study large variances in outcomes were seen among mice treated with ZA alone or in combination with PTH. This tends to suggest that the effectiveness of these therapies may depend on the degree of osteolysis present when treatment is initiated. Future studies will focus on treating each animal as a single patient with therapy initiated when osteolysis is positively identified on radiograph and changes in bone volume quantified by serial µCT.

Another limitation of this model is that µCT was not performed on the same bones used for mechanical testing. In order to obtain accurate measurements from µCT scans, the specimens need to be precisely aligned in the scanner. Although attempts were made to design alignment fixtures to support the entire mouse femur, it was not possible to consistently and accurately position the bones. Due to the fragility of the bones, the extra stress applied to them during alignment was enough to cause fracture. Therefore, direct correlations between bone strength and trabecular architecture could not be made on a bone-to-bone basis. However, the clear differences between the treatment groups with regards to both microarchitecture and bone strength suggest that loss of trabecular bone has a substantial effect on biomechanical strength. Future studies will focus on developing biomechanical testing protocols that can be performed in conjunction with µCT scans to allow direct correlations to be made between bone strength and trabecular architecture.

The study component using hPTH(1-34)NH$_2$ should be viewed as a proof of concept, rather than a pre-clinical test of a therapy that could be applied in a clinical setting. Clearly, hPTH(1-34)NH$_2$ cannot be used in cancer patients due to the potential risk of increased tumor growth and/or increased risk of osteosarcoma (21). However, hPTH(1-34)NH$_2$ is a potent anabolic agent and is an appropriate selection for a proof-of-concept treatment given its success in promoting bone accrual in the treatment of osteoporosis (18). However, due to the potential risk of increased tumor growth with PTH administration, we did not evaluate a 20Gy/PTH treatment group in this study. The four-week delay in administration of hPTH(1-34)NH$_2$ following radiation was used to reduce the risk of increased tumor growth that may be caused by hPTH(1-34)NH$_2$. Both radiation and zoledronic acid have been shown to induce apoptosis in breast cancer cells (19, 32, 38, 45, 74, 76, 77, 85). However, it should be noted that *in-vitro* studies indicate that it requires relatively high concentrations of zoledronic acid, in the range of 10-100 µM, to induce apoptosis in cancer cells. Even though the *in*-vivo plasma concentration of zoledronic acid is expected to be much lower, our treatment regime should significantly reduce the number of viable tumor cells prior to treatment with hPTH(1-34)NH$_2$. Although previous studies have shown that the effects of PTH (1-34) can be blunted when administered after the patient has been treated with a bisphosphonate (22, 35), these studies were performed within the context of osteoporosis rather than tumor osteolysis. Since the nature of the disease is quite different between osteoporosis and tumor-induced osteolysis, we sought to determine if hPTH(1-34)NH$_2$ could enhance bone quality and strength in our murine model of tumor-induced osteolysis.

The results of the current study provide insights into the relationship between bone quality and strength. Previous animal studies have demonstrated that osteolytic lesions treated with radiation therapy and/or a bisphosphonate are capable of regaining normal BMD and bone strength (11, 24, 50-52). However, it is well documented in osteoporosis literature that measures of BMD are not always predictors of bone strength (28, 41, 87). In the present study we demonstrated that although BMD and total bone volume were not significantly different from normal in tumor-burdened bones treated with radiation only, these bones were significantly weaker than normal femora. These results support the argument that BMD is a poor predictor of bone strength particularly in tumor osteolysis, where 3D microarchitectural changes are prominent. The addition of bisphosphonates alone or in combination with anabolic agents as adjuncts to

10

radiation therapy, appear to preserve trabecular architecture and maintain or increase bone strength. Taken together, these results support the hypothesis that trabecular architecture is a major contributor to bone strength (41), and that excessive thinning or loss of connectivity predisposes the bone to fracture (3, 4, 80). Through this study, we are able to begin to understand why clinical lesions treated with radiation therapy remain at high risk for pathological fracture (47) and that adjuvant treatment with antiresorptive agents alone or in combination with anabolic agents may reduce fracture risk by restoring or maintaining trabecular bone. Future studies should focus on developing techniques to correlate trabecular bone architecture and biomechanical strength.

2.2: *Task 2: To evaluate the response of tumor-burdened bone to treatment with zoledronic acid and to determine whether microarchitecture and biomechanical strength can be restored to normal*

Pre-clinical animal models play a critical role in increasing our understanding of human diseases and in developing therapies to treat these diseases. These models also aid in the development of new imaging technologies that can be used in the clinical setting. Some diseases that rely heavily on imaging techniques to monitor disease progression and therapeutic efficacy include osteoporosis, arthritis, heart disease, and cancer. Several imaging techniques are currently available for use in a pre-clinical setting, ranging from X-rays and DEXA scans to more sophisticated techniques that involve the imaging of fluorescent molecular probes and bioluminescent tumor cells (31). In the course of this dissertation we have explored the use of some of these technologies in our mouse model of tumor-induced osteolysis. In this chapter we would like to discuss the development of our *in vivo* µCT protocol.

Accurate quantification of bone loss and changes in bone microarchitecture are critical for assessing the efficacy of anti-resorptive and anabolic agents used to treat bone loss. In addition, these measurements can potentially be used as surrogates for estimates of bone strength. Prior to the development of µCT scanners, changes in bone density and morphology were measured using dual energy X-ray absorptiometry (DEXA), peripheral quantitative computed tomography (pQCT), X-rays, and histology. DEXA and pQCT scans allow for quantification of relative changes in bone density, but do not allow assessment of total bone volume or trabecular microarchitecture. However, these techniques are non-invasive and can be repeated throughout the course of a study on the same animal. Although X-rays can also be obtained serially and are capable of depicting the progression of bone loss, it is difficult to accurately and objectively quantify these changes. Histology has been the gold standard for assessing total bone volume and quantifying trabecular microarchitectural properties. However, this technique is destructive to the tissue and can only be performed on post-mortem samples. In addition, histology is very time consuming and can become increasingly more difficult to perform as the degree of bone destruction increases. Although these techniques provide a metric for monitoring bone destruction over time and quantification of bone loss at the end of the study, they are not amenable to detecting changes in bone structure over time in response to disease and/or therapy. And possibly even more importantly, they do not provide a way to correlate changes in bone morphology with bone strength. Although histology can technically be performed on mechanically tested bones, the resulting morphology will not accurately represent the structure of the bone at the time of testing.

The development of *in* vivo µCT scanners has addressed some of the limitations associated with DEXA, pQCT, X-ray, and histology. Additionally, *in-vivo* whole-body CT scans of a mouse can be equated to whole-body human CT scans used clinically. Development of a pre-clinical model, in which serial CT scans could be correlated to fracture risk would therefore be easily translated into clinical practice. The goal of this pilot study was to develop a protocol to image tumor-burdened femora using an *in-vivo* µCT scanner and to assess whether serial scans could be used to quantify the progression of tumor-induced osteolysis and response to therapy. In an effort to be more clinically relevant, we sought to treat each mouse as an individual patient, initiating treatment only when osteolysis was detectable on X-ray. In addition, we wanted to be certain that we were consistent in administering therapy as a treatment for an established lesion, rather than as a preventative measure. Using this approach, we hypothesized that *in-vivo* CT scans taken when osteolysis was first detected on radiograph and again four weeks later would demonstrate a significant decrease in total bone volume and bone mineral content. In addition, we

11

hypothesized that bones treated with zoledronic acid, starting the day of the first CT scan, would exhibit improved bone volume and mineral content and decreased osteolysis compared to untreated bones.

Materials and Methods

Study Design

The right femur of 20 female nude mice was injected with human breast cancer cells as previously described (2). The development of osteolytic lesions was monitored by weekly X-rays and a radiographic scoring scheme (90) was implemented as a screening modality to identify mice with established lesions. In this study, when a mouse received a score of 1 to 2, it was selected to start treatment (zoledronic acid or saline) and was scanned on the *in-vivo* µCT scanner. Mice were treated once-weekly for four weeks and then euthanized. However, if a mouse displayed severe osteolysis (lysis score of 4) it was euthanized immediately. All mice were then scanned a second time on the *in vivo* µCT scanner. 3D reconstructions of the initial and final bone scans were created and total bone volume and mineral content were calculated. All experimental procedures used in this study were reviewed and approved by the local IACUC.

Tumor Cells

F10 cells, a bone-adapted clone derived from the human MDA-MB-231 breast carcinoma cell line (92) (Dr. Toshiyuki Yoneda, UT San Antonio, TX) were used for this study. Cells were cultured in Dulbecco's modification of Eagle's medium (DMEM) supplemented with 10% (v/v) fetal calf serum (FCS) and 1% penicillin-streptomycin-glutamine (Gibco, Grand Island, NY) and maintained at 37ºC in an atmosphere of 5% CO_2 in air.

Tumor Cell Inoculation

Female NCr homozygous nude mice (8 to 9 weeks old, 20-25 grams body weight, n=20) (Charles River, Wilmington, MA) were anesthetized with an injectable drug cocktail consisting of Telazol$^®$ (45mg/kg, IM) and xylazine (7.5 mg/kg, IM). A small incision was made at the knee joint and the patella carefully moved to expose the distal end of the femur. Using a sterile 26G needle, twenty microliters of cell suspension (containing 1 x 10^5 F10 breast cancer cells) were injected through the intercondylar fossa of the right femur to a depth of approximately 5 mm. The contra-lateral limb served as an internal control. Mice were housed in micro-isolators with a 12-hour day/night cycle and were fed a diet of autoclaved food and water *ad libitum*.

Radiographic Evaluation of Osteolysis

Lateral radiographs were obtained weekly starting at time of surgery using a Faxitron MX-20 (Faxitron X-ray Corporation; Buffalo Grove, IL) and MIN-R 2000 mammography film (Kodak; Rochester, NY). A standardized scoring system was used to evaluate radiographic lesions in the femur. A grade of zero represented no lysis, 1+ indicated minimal but detectable lysis within the medullary canal, 2+ represented moderate lysis limited to the medullary canal, 3+ reflected severe medullary lysis with cortical involvement and 4+ indicated massive lysis with cortical destruction and soft tissue extension (90).

Treatment Schedule

Following radiographic evaluation, mice that received a score of 1 to 2 were selected to start therapy. Mice were randomly allocated for treatment with 100 µl of saline or 25 µg/kg of zoledronic acid (ZA, Novartis, Switzerland) once weekly for four weeks.

In-vivo µCT Scanning

Mice were scanned on a MicroCAT II (Siemens Preclinical Solutions, Malvern, PA). In an effort to reduce the number of scans and scan time, a customized sled was designed on which two mice could be placed tail-to-tail. Using this setup, only the caudal-half of each mouse was included in the scan region. This reduced the amount of radiation exposure to the whole animal, while allowing for increased resolution. X-ray acquisition settings were 80 kVp and 500 µA with an integration time of 400-ms. Scans were performed with an isotropic voxel size of 42 µm.

12

For the survival scans, mice were anesthetized with an injectable drug cocktail consisting of Telazol® (45mg/kg, IM) and xylazine (7.5 mg/kg, IM) in a laminar flow hood. The sled and scanning tube were disinfected in between each scan. A custom foam support was placed between the legs of each mouse in an effort to keep the hind limbs flexed and parallel to one another. Mice were then taped to the sled using 3M transpore tape and the sled was placed inside the scanning tube. A thin wire heating pad was placed underneath the sled to keep the mice warm during the scan session, which lasted approximately 32 minutes. Terminal scans were performed post-mortem and mice were simply taped to the sled and placed inside the scanning tube.

Axial scan slices were imported into Mimics 3D reconstruction software (Materialise US, Ann Arbor, MI). A hydroxyapatite (HA) phantom was used to calibrate gray-scale levels, and a threshold of 400 mg/cc HA was used to distinguish bone from surrounding tissue. The distal 5 mm of the femur was then isolated for both the normal and tumor bearing limbs. The average HA density and total bone volume (BV) for each femur was then determined. Bone mineral content (BMC) was calculated by multiplying the total bone volume by the HA density.

Statistics
Analysis of variance (ANOVA) with a Fisher's PLSD *post-hoc* was performed to determine differences between groups and a paired t-test was performed to determine differences between the initial and terminal µCT scans. Significance was taken at $p < 0.05$.

Results
Tumor Engraftment and Survival
All of the mice survived surgery with no complications. At seven day post-tumor injection, one mouse died while anesthetized for X-ray. An additional, two mice did not survive their first *in-vivo* µCT scan due to anesthesia. At six weeks, four mice showed no signs of osteolysis on radiograph and were excluded from the study. At three weeks post-tumor injection, eight mice displayed lytic lesions with a score of 1 or 2. At four weeks, four more mice had established bone lesions, and at five weeks the remaining three mice had identifiable lytic lesions (Figure 2.1). All mice were euthanized by six weeks after tumor injection due to completion of drug therapy or severe osteolysis.

Assessment of Total Bone Loss
Total bone volume was 18% lower in tumor bearing bones compared to normal bones at the start of treatment (p<0.0001) (Figure 2.2). There was no difference in BV between mice selected for treatment with vehicle or ZA, both at the start of treatment and at the end of the study (p=0.988 and p=0.454, respectively) (Figure 2.5). A similar trend was seen for BMC (Table 2.1). At the end of the study, tumor bearing femora displayed an average 35% decrease in BV compared to the normal limb (p<0.0001) (Figure 2.3). This represents an additional 15.7% decrease in BV compared to the initial scan (p=0.0184). Although not statistically different, mice treated with ZA appeared to lose bone at a slower rate (0.06 mm^3/day ± 0.10) compared to vehicle treated mice (0.20 mm^3/day ± 0.17) (p=0.095).

Treatment with Zoledronic Acid does not Reduce Fracture Risk
In this study seven mice were treated with zoledronic acid and eight were treated with vehicle (saline). Of these mice, only two in the ZA treatment group survived long enough to receive all four doses of drug. Of the mice treated with vehicle, none of them survived beyond five weeks post-tumor injection (Figure 2.4). 3D reconstructions of the femora revealed that four of the vehicle treated mice and six of the ZA treated mice had completely fractured. Two of the mice treated with ZA demonstrated an apparent increase in BV. 3D reconstructions revealed that osteolysis was still occurring in the metaphyseal region; however cortical thickness appeared to be increasing (Figure 2.5).
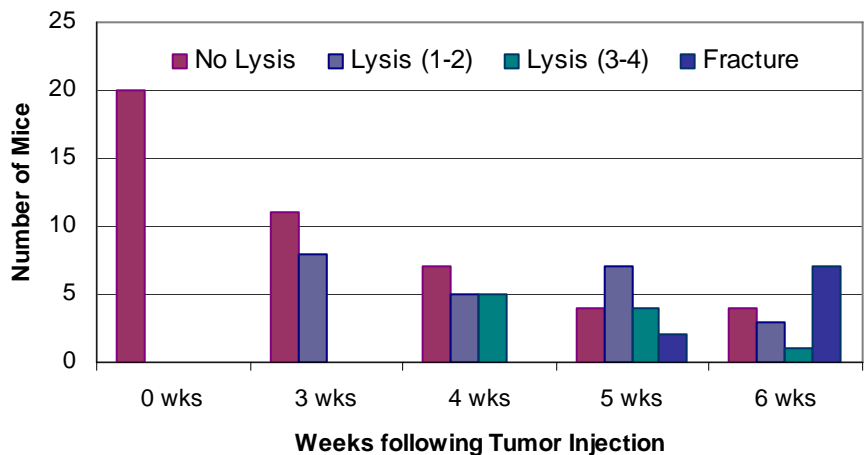
13

Figure 2.1: Development and Progression of Osteolysis
Mice were injected with tumor at week 0. Following weekly X-rays, mice were assigned to vehicle or ZA when they developed a lytic lesion. Mice were treated for 4 weeks and then euthanized. 63% of the mice developed lesions between 3 and 4 weeks following tumor injection. By 6 weeks, 69% of the mice with successful tumor engraftment were taken off study due to impending fracture. Four mice did not develop lesions.

Table 2.1: Bone Mineral Content in the Distal 5 mm
There was no significant difference in BMC between mice assigned for vehicle or ZA treatment. Terminal BMC did not increase with ZA treatment. (Significance taken at $p<0.05$)

		Bone Mineral Content (mg)		
Time Point	Treatment	Mean	SD	ANOVA (p-value)
Initial	Vehicle	5.75	0.97	0.894
	ZA	5.68	0.82	
Terminal	Vehicle	4.47	1.6	0.435
	ZA	5.33	2.1	

14

Effect of ZA on Normal Bone Volume

Changes in total BV could also be detected in the normal limb of mice treated with ZA. At the end of the study, these mice displayed an average 8% increase in BV compared to their initial scan (p=0.028). Mice that were treated with vehicle had an average 3% increase in BV, but this was not significant (p=0.287). Therefore, it appears that ZA affects the bone volume of normal bones and this can be detected by temporal *in vivo* CT scans.

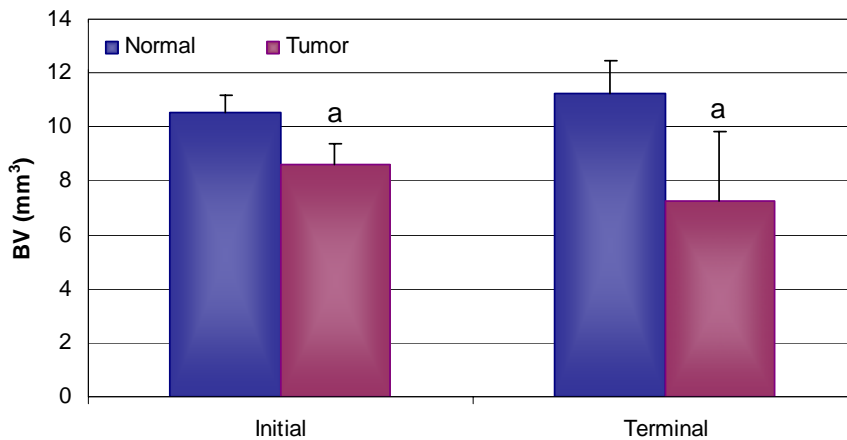**Figure 2.2: Total Bone Volume in the Distal 5 mm**
There was a significant decrease in BV between normal and tumor bearing femora at the start of treatment and at the end of the study.
a = significant from normal
Significance taken at p<0.05

15
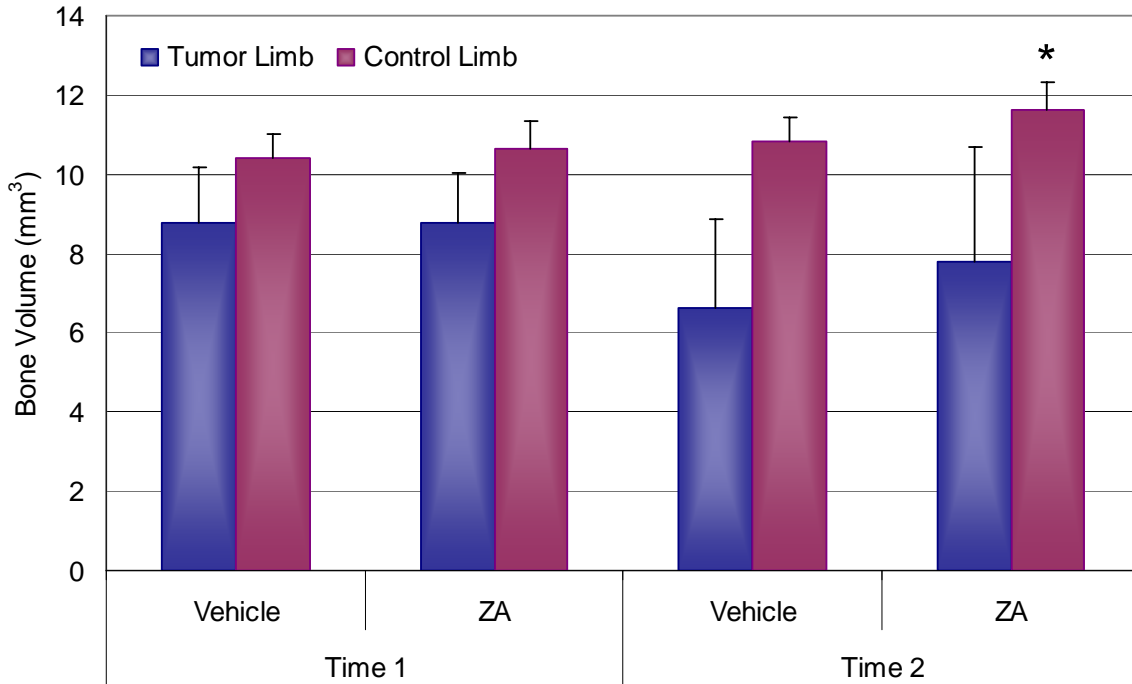
Figure 2.3: *In Vivo* Measure of Bone Volume
There was not a significant difference in BV between mice treated with vehicle or ZA at the start of treatment or at the end of the study. The control limb of the ZA treated mice displayed an 8% increase in total BV (p=0.028).

Figure 2.4: Progression of Impending Fracture Based on Treatment
One mouse died at seven days with no lysis. Four ZA mice were euthanized at 35 days due to impending fracture. Two mice treated with vehicle died during micro-CT scanning. By six weeks following tumor-injection, all mice treated with vehicle were euthanized due to severe osteolysis and impending fracture.

16

Figure 2.5: 3D Reconstructions of the Distal 5 mm of the Femur
Total bone volume (BV, mm^3) was determined for the distal 5 mm of the femur. Osteolysis increased from the initial scan to 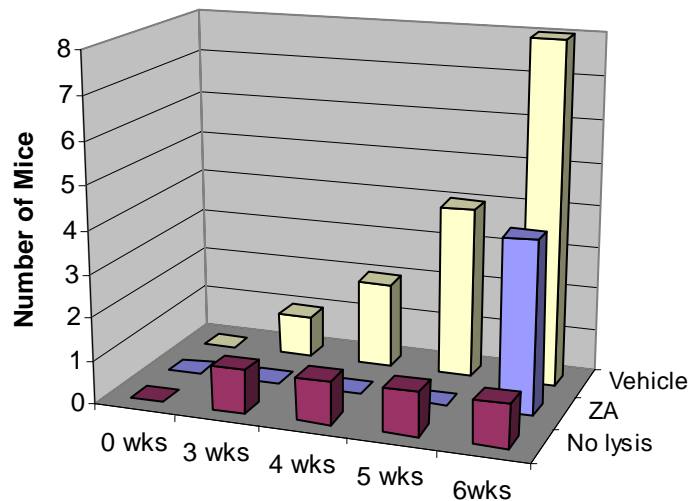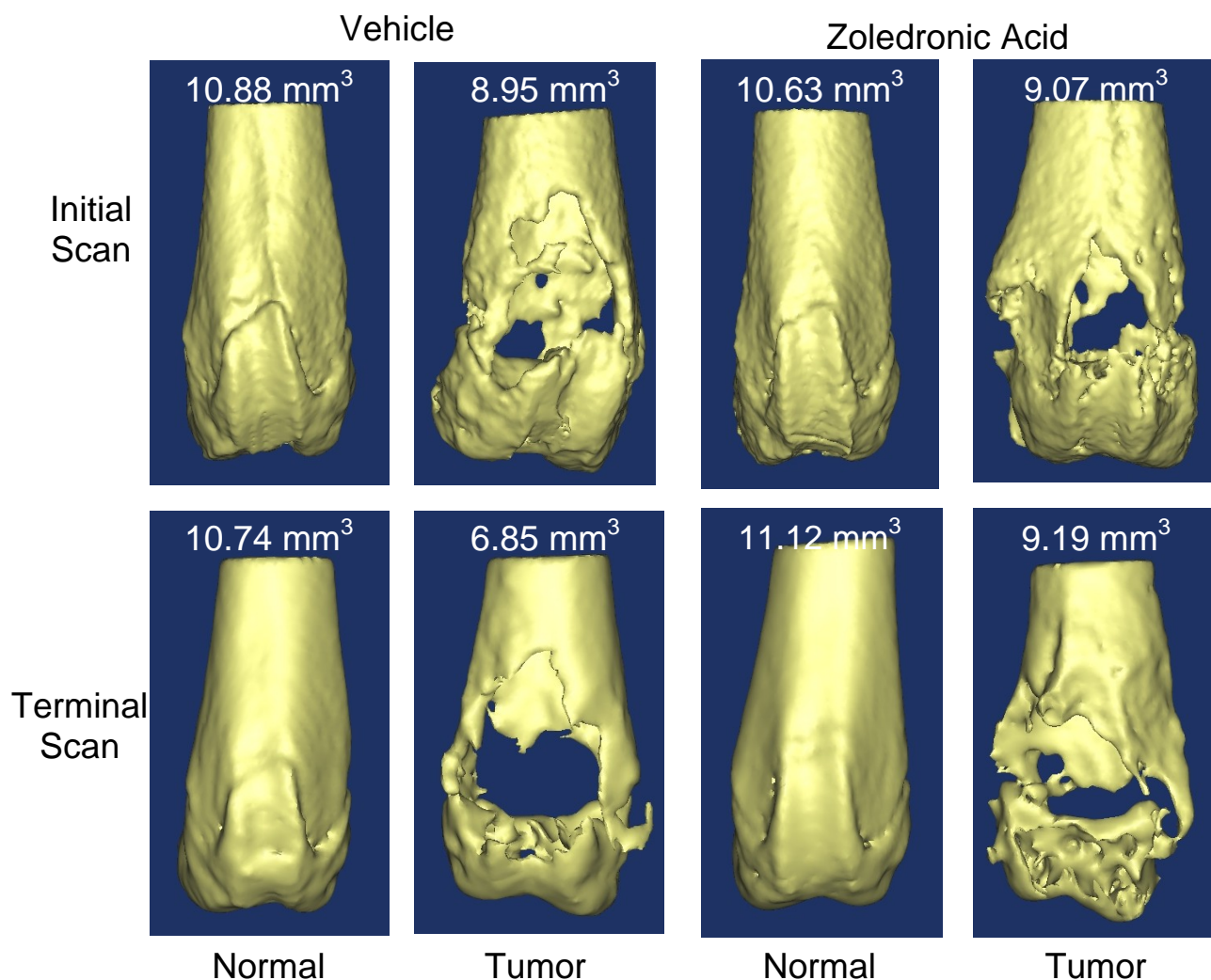the terminal scan in both vehicle and ZA treated mice. However, two mice treated with ZA displayed an apparent increase in BV, which may be attributed to increased cortical thickness. Non-tumor bearing bones exposed to ZA also exhibited increased BV (p=0.028).

Discussion
In vivo μCT scanners have the potential to provide accurate measurements on temporal changes in total bone volume due to disease and treatments, while reducing the number of animals. In this study we have shown that although mice were selected on the basis radiographic evidence of osteolysis, there was still significant variation between animals at the start of treatment. However, we were able to achieve equal distribution of osteolysis between the vehicle and ZA treatment groups. Weekly *in-vivo* scans would provide a more accurate measure of disease progression; however this approach is not feasible in the laboratory or the clinic. Despite this limitation, we were also able to demonstrate that total bone volume and bone mineral content significantly decreased from the start of therapy to the end of the study based on *in-vivo* μCT data. In addition, we were able to detect an 8% increase in BV in normal limbs exposed to ZA. Therefore, these results confirm that small changes in bone volume can be distinguished using an *in-vivo* μCT scanner.

17

However, this model has some limitations. Mouse trabeculae are approximately 50 microns in diameter and the highest resolution that we could safely obtain with the *in-vivo* scanner was 42 microns. This means that we are limited to measurements of total bone, and assessment of trabecular microarchitecture would have to performed post-mortem on *ex-vivo* specimens. Another limitation is the dose of radiation the mice are exposed to during the scan, which can alter immune responses and biological pathways (8). The dose of radiation is dependent on the X-ray settings (kV, µA), acquisition time, number of projections, and specimen diameter. Depending on the scan conditions, the radiation dose has been measured to range from 0.44 mGy to 0.25 Gy (8, 9, 56). The total accumulated absorbed radiation dose an animal will be exposed to will depend on the total number of serial scans. Multiple radiation exposure may have an impact on tumor cell survival. Therefore, when conducting experiments looking at various therapies to treat tumor-induced osteolysis, the effect of radiation dose and exposure must be taken into account. Future studies utilizing our model should include a measurement of radiation dose delivered to the whole animal as well as the bone.

The tumor cell line used in this experiment was also very aggressive, preventing most mice from surviving past 6 weeks after tumor-injection. This prevented most of the ZA treated mice from receiving the full course of the drug. However, our results tend to suggest that if the tumor burden is not controlled; ZA alone is not capable of preventing tumor-induced osteolysis. These results are consistent with previous work on neuroblastoma cells, where mice with established osteolytic lesions and treated with ZA continued to lose bone (69). In order for patients with established lytic bone lesions to benefit from the antiresorptive properties of bisphosphonates, ZA should be combined with a tumoricidal agent. Our results also show that the rate of tumor growth and destruction varies greatly between animals. Therefore larger group sizes may be required to establish the efficacy of therapeutic treatments.

The development of this *in-vivo* µCT protocol using our established mouse model of tumor-induced osteolysis provides an ethical and cost-effective way to evaluate the effect of therapy on the progression of osteolysis. Serial scans can be taken over time of the same animal, thereby reducing the number of animals required as well as improving statistical power through use of repeated measures. Since CT scanning is a non-invasive technique, the same bones can be further analyzed for biomechanical testing or histomorphometric analysis. Future studies will focus on incorporating the use of *in-vivo* µCT scanning into our validated methodologies to test the efficacy of clinically relevant therapies for treating tumor-induced osteolysis. This approach also could be used to test predictive capabilities of bone strength surrogates such as DEXA (BMD), sectional analysis or finite element methods. As the relative resolution of this approach for the mouse model is similar to the human CT scanners, this would serve as an appropriate tool for developing this methodology.

2.3: *Task 3: Effect of radiation and ZA on Osteoblasts, Mesenchymal Stem Cells, and Breast Cancer Cells In-Vitro*

In addition to bisphosphonate therapy, many patients with bone metastases are treated with radiotherapy to control tumor burden and bone pain (36). Recent *in-vitro* studies have shown radiation and zoledronic acid (ZA) appear to have a synergistic cytotoxic effect on breast and prostate cancer, as well as myeloma (1, 85). These studies have shown that to achieve a 50% decrease in cell viability, high doses of ZA (~100 µM) are required. However, pharmacokinetic studies have demonstrated that the plasma concentration of ZA in human patients treated with 4 mg ZA is around 2 µM 24 hours following infusion (79). Based on these preliminary studies, we wanted to further explore the effect of ZA and radiation on the F10 breast cancer cell line. In addition, little is known about the effect of radiation and ZA on osteoblasts and bone marrow stromal cells, which play crucial roles in maintaining the bone microenvironment. Therefore, the specific aim of this study was to determine the sensitivity of osteoblasts and marrow stromal cells to radiation, ZA and the combination of radiation plus ZA with respect to metastatic breast cancer cells. We hypothesized that breast cancer cells would be more sensitive to radiation and less sensitive to zoledronic acid, compared to either osteoblasts or marrow stromal cells. In addition we hypothesized that continuous exposure to zoledronic acid, administered before radiation therapy, would radiosensitize the breast cancer cells causing increased cell death. Further more, we

18

hypothesized that radiation plus ZA would have little effect on osteoblasts and marrow stromal cells compared to treatment with radiation alone.

Materials and Methods

Cell Lines and Culture Conditions

F10 cells, a bone-adapted clone derived from the human MDA-MB-231 breast carcinoma cell line (93) (Dr. Toshiyuki Yoneda, UT San Antonio, TX), and ST2, immortalized mouse stromal cells, were cultured in Dulbecco's modification of Eagle's medium (DMEM). MC3T3 subclone 4 cells, an immortalized mouse osteoblast-like cell line, were cultured in ascorbic acid-free alpha modification of Eagle's medium (alpha-MEM). Primary mouse marrow stromal cells (MSCs) were cultured in a 50/50 (v/v) of MesenCult and DMEM. DMEM and alpha-MEM (Gibco, Grand Island, NY) were supplemented with 10% (v/v) fetal calf serum (FCS) and 1% penicillin-streptomycin-glutamine. MesenCult MSC Basal medium (mouse) was supplemented with mesenchymal stem cell stimulatory supplement (mouse) (Stem Cell Technologies, Vancouver, CA). All cells were maintained at 37ºC in an atmosphere of 5% CO_2 in air. Culture media was change twice a week. Cells were split at 90% confluence using trypsin EDTA, 1x (Cell Grow, Mediatech, Herndon, VA) to remove them from the flask.

Radiation Therapy

Radiation was administered with a Phillips MGC-30 therapeutic X-ray machine operating at 300 kilovolts and 10 milliamps (effective dose rate 2.04 Gy/minute at a source-to-object distance of 15 cm). Cells were irradiated 24 hours after cell seeding.

Zoledronic Acid

Zoledronic acid (ZA) was obtained in the form a disodium salt from Novartis, Pharma AG (Basel, Switzerland). A 500-µM stock solution was prepared and sterile filtered through a 0.22-µm filer and stored in 2-ml aliquots at -20°C until use. Zoledronic acid dilutions (0.05 - 100 µM) were prepared in media immediately before use.

Cell Viability

Clonogenicity Assays

Cells were seeded at a density of 100 to 10,000 cells/well in 6-well plates. After 24 hours, plates were irradiated with 0, 1, 2, 4, 5, 8, 10, and 20 Gy. Cells were cultured for 7 to 10 days without media changes until identifiable clones were present. Colonies were fixed with ice-cold 70% ethanol, stained with 2% crystal violet, and counted. Log-lin plots of survival fraction versus radiation dose were constructed and the D_0 values (a measure of radiation sensitivity, 37% cell survival) were determined.

MTT Assay

Cells were seeded at 5×10^4 cells/well in 24-well plates. 24 hours after seeding, cells were treated with radiation and/or ZA with no washout. At 3 and 7 days following treatment MTT (3-[45-dimethyl-thiazoyl]-2,5-diphenyl-tetrazolium bromide (Sigma, St. Louis, MO) colorimetric assays were performed to assess cell viability. 100-µl yellow MTT solution (5 mg/ml) were added to each well, and the plates were further incubated at 37°C and 5% CO_2 to allow healthy mitochondria to metabolize the dye and form dark blue thiazol crystals. After 60 minutes, the media was aspirated and 500 µl of DMSO was added to each well to dissolve the crystals. The absorbance was read on a spectrophotometer (Wallac Victor^2 1420 multilabel counter, Turku, Finland) at a wave length of 560 nm. Approximate IC_{50} values were determined from 7 day MTT results by interpolating the concentration at which cell viability was reduced to 50% of the control.

Detection of Apoptosis

RT-PCR

RT-PCR was performed to study the effect of radiation therapy and zoledronic acid, alone or in combination, on the expression of Bax and Bcl-2, known regulators of apoptosis. Cells were seeded in T-75 culture flasks and were treated 72 hours later when cells were approximately 80% confluent. Cells were treated with 10 Gy radiation (10Gy), 5 µM ZA (ZA), or 5 µM ZA followed by 10Gy radiation

19

(10Gy+ZA). Forty-eight hours following treatment, culture media was aspirated, cells were washed in PBS, and then lysed with RTL buffer containing 0.01% β-mercaptoethanol. The lysates were then homoginzed using a Quiashredder column, and total RNA was extracted with on-column DNase treatment using an RNeasy kit (Qiagen, Valencia, CA). The resulting extract was then analyzed by UV-absorbance spectrophotometry to determine the quantity (280 nm, 1.0 AU = 40 µg/ml) and purity (ratio of absorbance at 260 nm and 280 nm) of each RNA sample. Using 1 µg of total RNA, the mRNA fraction of the extract was selectively reverse-transcribed using oligo-(dT_{15}) primers and Moloney-murine leukemia virus reverse transcriptase to produce template cDNA polymerase (Promega, Madison, WI). HotStar Taq Plus DNA polymerase (Qiagen, Valencia, CA) and gene specific oligonucleotide primers (MWG Biotech, High Point, NC) were used to probe the expression level of Bax, Bcl-2, and β-actin transcripts by polymerase chain reaction (PCR) using 0.5 µl of cDNA template (Table 3.1). The products of the PCR reactions were then resolved by electrophoresis through a 3% agarose-TBE gel, stained with ethidium bromide and digitally imaged under long-wave UV illumination. The expected product size was verified by comparison of the migration of the apparent product relative to the migration of a 100 bp DNA standard ladder (Bench Top 100 bp, Promega, Madison, WI).

Table 3.1: cDNA Templates for Bcl-2, Bax, and β-actin

Gene	NCBI Accession	Sense Primer (5'-3')	Antisense Primer (5'-3')	5'-3' mRNA Position	Product Size	# PCR Cycles	Anealing Temp. (°C)
Bcl-2	NM_009741.3	ctgcaaatgctggactgaaa	ccagattgggtcctcacact	566-711	146 bp	32	55°C
Bax	NM_007527.3	tgcagaggatgattgctgac	gatcagctcgggcactttag	350-522	173 bp	27	55°C
β-actin	NM_007393.3	aggtatcctgaccctgaagt	aggtctcaaacatgatctgg	265-458	194 bp	25	53°C

Western Blot
Western blots were performed to evaluate protein expression of Bax. Cells were seeded at $1x10^5$ cell/well in a 6-well plate and treated with 0Gy, 5 µM ZA, 10Gy, or 10Gy+ 5 µM ZA 24 hours after seeding. Two days following treatment, the media was aspirated and the cells were washed with cold PBS and 150 µl of lysis buffer was added to each well. The cells were collected and centrifuged at 10,000 RPM for 5 minutes at 4°C. The supernatent containing the protein was then collected and stored at -20°C. Protein concentration of cell lysates was measured using a BCA total protein assay (BCA Assay; Pierce, Rockford, IL). Equal amounts of protein sample was loaded on a SDS-PAGE gel (Bio-Rad, Hercules, CA) and Bax P-19 antibody (Santa Cruz Biotechnology, Santa Cruz, CA). Specific protein bands were visualized by ECL kit (Pierce, Rockford, IL) after being probed with a secondary HRP-conjugated antibody.

Colorimetric Assay
Apoptosis was quantified by the proteolytic cleavage of the caspase-3 substrate Z-DEVD-AMC using the EnZCheck Caspase-3 Assay kit (Invitrogen, Eugene, OR). Cells were seeded at $5x10^4$ cells/well in a 24-well plate and treated with radiation, ZA, or radiation+ZA 24 hours after seeding and incubated for an additional 48 hours. Fluorescence was measured using a spectrophotometer at an excitation of 360 nm and emission of 465 nm.

Caspase activity was normalized to total protein concentrations measured with a BCA total protein assay (BCA Assay; Pierce, Rockford, IL). Briefly, 50 µl of cell lysate or 50 µl of standard were added to a 96-well plate in duplicate. 50 µl of BCA reagent were then added to each well and the plate was incubated at room temperature. Optical density was read at 562 nm. Protein-normalized caspase values were then normalized to control samples to determine relative changes in caspase activity between treatments.

Immunohistochemistry
Cells were seeded at $5x10^4$ cells/well on sterile glass disks (12cm) in 24-well plates. Twenty-four hours after seeding cells were treated with radiation, ZA, or radiation+ZA. Forty-eight hours after treatment cells were fixed in a 4% parafomaldehyde, 2% acetone, and 2% methanol (v/v) in PBS (pH 7.1) fixative for 3

hours and then in 70% ethanol over night. Cells were washed in PBS and then incubated in 500 µl of citrate buffer for 30 minutes at 50°C. The citrate buffer was removed and the cells were incubated in 500 µl of 1% BSA for 30 minutes at room temperature. 2 µl of full-length, caspase-3 antibody (Trevisen, Gaithenburg, MD 1:250) was added to each well and incubated for at least 1 hour at room temperature. Cells were then washed 3 times in PBS and 500 µl of 1% BSA, 2 µl of Alexa Fluor 568 (rabbit raised in goat, Molecular Probes, Eugene, OR), and 5 µl of DAPI (100 µg/ml, Sigma) was added to each well. Cells were then incubated for at least 1 hour at room temperature, shielded from light. Glass disks were then placed on slides and viewed using a G-2A ban-pass filter (excitation 510-560 for caspase) and a UV-1A ban-pass filter (excitation 355-375 for DAPI) on a Nikon Eclipse E400 microscope.

Annexin V/PI staining

Apoptosis was also confirmed in the F10 cell line using annexin-V/propidium iodide staining (Calbiochem, LaJolla, CA). During the early stages of apoptosis, the dying cell's membrane undergoes changes resulting in the expression of a phospholipid-like phosphatidyl-serine (PPS) membrane protein. Annexin V is a Ca^{2+}-dependent phospholipids-binding protein that has a high affinity for PPS. To detect this early stage of apoptosis, F10 cells were seeded at $5x10^4$ cells/well in a 24-well plate and treated with 0Gy, 5 µM ZA, 10Gy, or 10Gy+ 5 µM ZA 24 hours after seeding. Two days following treatment the media were collected and the cells were trypinsized and placed in the corresponding tube. Cells were counted and adjusted to $1x10^6$ cells/ml and re-suspended in 500 µl of PBS. Ten microliters of media binding agent was added to each tube followed by 1.25 µl of Annexin V-FITC. Tubes were then incubated in the dark for 15 minutes. Cells were centrifuged for 10 minutes at 1000*g* at room temperature. The media was aspirated and 500 µl of cold 1X binding buffer was added followed by 10 µl of propidium iodide. Samples were then placed on ice and immediately observed at 488 nm on a FACStar$^+$ argon laser flow cytometer (Becton Dickinson, Franklin Lakes, NJ). The spectrophotometric values measured for ten thousand cells were analyzed using Flowjo (Tree Star, Ashland, OR). Unstained, FITC only, and PI only untreated cells were used to determine compensation.

Cell Cycle Analysis

Cells were seeded at $5x10^4$ cells/well in a 24-well plate and treated with 0Gy, 5 µM ZA, 10Gy, or 10Gy+ 5 µM ZA 24 hours after seeding. Two days following treatment the media were collected and the cells were trypinsized and placed in the corresponding tube. Cells were counted and adjusted to $1x10^6$ cells/ml and washed in ice-cold PBS and centrifuged at *1000g* three times. After the final spin in PBS, cells were resuspended in 70% ethanol where they could be stored over night at -20°C. Cells were then spun down and washed once in PBS and then resuspended in 500 µl of RNase A (2 mg/ml) and incubated for 30 minutes at 37°C. Following incubation, cells were stained with 500 µl of propidium iodide (50 µg/ml, Sigma) for 30 minutes. Samples were kept on ice and immediately observed at 488 nm on a FACStar$^+$ flow cytometer and analyzed using Flowjo (Tree Star, Ashland, OR) to determine the percentage of cells in the G_0/G_1, S, and G_2/M phases of the cell cycle.

Mineralization

MC3T3 (immortalized mouse osteoblast-like cells) and MSC (primary mouse marrow stromal cells) were seeded at a density of $1x10^5$ cells/well in 6-well plates. Once the cultures were confluent (3-4 days), the medium was replaced with mineralization media containing ascorbic acid (100 µM) and sodium phosphate (5 mM). Cells were then treated with 0Gy, 5 µM ZA, 10Gy, or 10Gy+ 5 µM ZA, and cultured for 21 days to allow mineral formation. Media changes took place twice a week and were supplemented with ascorbic acid, sodium phosphate, and where appropriate, ZA. At 21 days the medium was aspirated, cells were washed with PBS and fixed in ice-cold 70% ethanol for one hour. The cells were then rinsed with deionized water and stained with Alizarin Red S (40 mM, pH 4.2, Baker Analyzed, Phillipsburg, NJ) for 10 minutes. Plates were then rinsed five times with DI water and washed in PBS for 15 minutes with rotation. Plates were photographed and then destained with cetylpyridinium chloride solution (MP Biomedicals, LLC, Solon, OH; 10% w/v in sodium phosphate, pH 7.0) for 30 minutes. Standards were prepared by diluting the Alizarin Red S solution in cetylpyridinium chloride solution (0-1.6 mM dilutions) 100 µl of standard or sample was added in duplicate to a 96-well plate and the optical density read at 562 nm.

21

The results are presented as a percentage of control, non-treated cells. All experiments were repeated on three separate occasions. All data, except Annexin V/PI were analyzed by analysis of variance (ANOVA) along with Fisher's PLSD post-hoc. Statistical significance was taken at $p < 0.05$.

Results

Cellular Sensitivity to Zoledronic Acid and Radiation

Treatment of MC3T3, ST2, MSC, and F10 cells with increasing concentrations of ZA caused dose- (Figure 3.1) and time-dependent decreases in cell viability at three and seven days. ZA (1-25 µM) had little effect on F10 cells at three days, however cell viability decreased 15% compared to the untreated control at 7 days when treated with 1 µM ZA (p=0.011) (Figure 3.2). Cell viability was significantly decreased in both the MC3T3 (p=0.001) and MSC (p<0.0001) cells at three days compared to the untreated control at concentrations of 5 µM or higher. Cell viability was assessed at seven days in ST2 cells exposed to increasing doses of ZA (0.05 to 20 µM). At a concentration of 0.05 µM, ST2 cells exhibited a 12.7% decrease in cell viability compared to control (p<0.0001). The approximate IC_{50} values at seven days were 39 µM for F10 cells, 30 µM for MSC cells, 14 µM for MC3T3 cells, and 7 µM for ST2 cells. Clonogenic assays were performed to establish intrinsic cellular radiosensitivity. The D_0 values (37% cell survival) were calculated to be 2.4 Gy for F10 cells, 5.8 Gy for MC3T3 cells, and 3.0 Gy for ST2 cells.
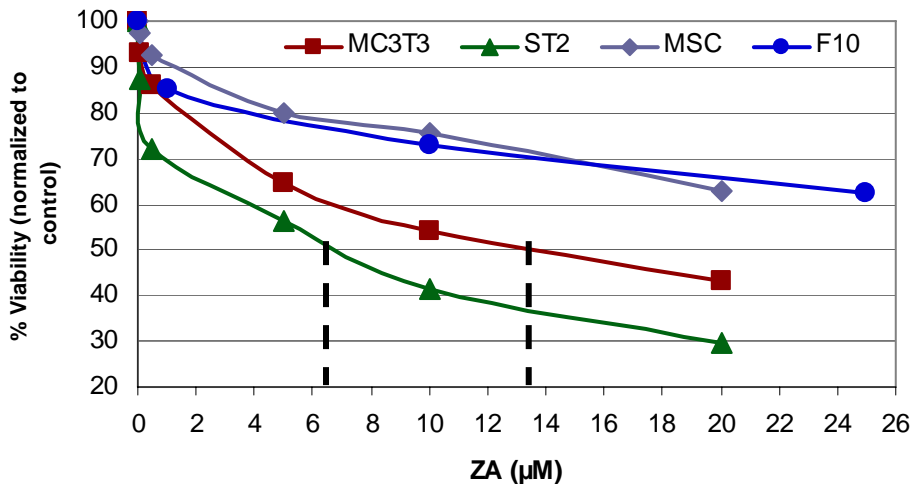
Figure 3.1: Effect of ZA on Cell Viability at 7 Days. Chronic exposure to zoledronic acid (0 to 25 µM ZA) for 7 days caused a dose-dependent decrease in cell viability. MSC and F10 cells do not appear to be as sensitive to ZA as ST2 and MC3T3 cells.

Figure 3.2: Effect of ZA on F10 Cell Viability at 3 and 7 Days Cell viability decreased with increasing chronic exposure to zoledronic acid (0 to 100 µM ZA). Based on these results, F10 cells require chronic exposure to 39 µM of ZA for 7 days to decrease cell viability by 50%.

Effect of Radiation and Zoledronic Acid on Cell Viability

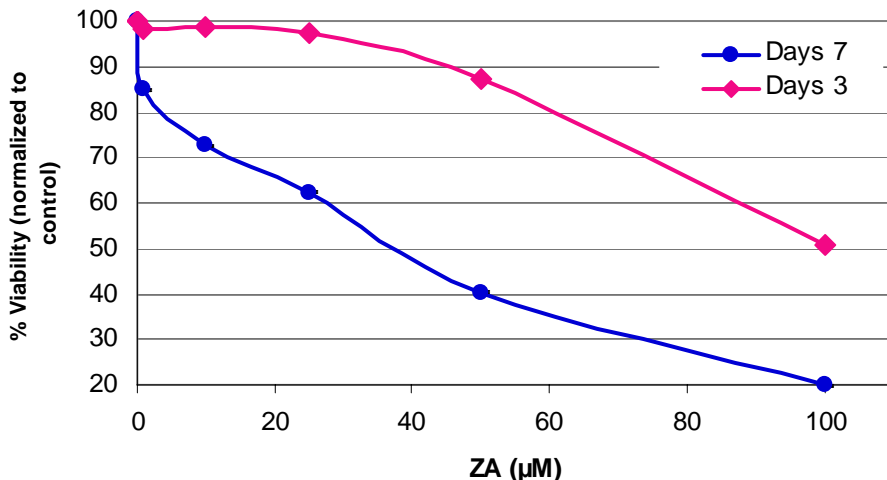The actual concentration range of zoledronic acid that cells would be exposed to *in vivo* is unknown. In human patients treated with the standard 4 mg dose of ZA, the maximum plasma concentration achieved was 1 µM (79). In a rat model, where 0.16 mg/kg of ZA was administered i.v., plasma concentrations reached 4.47 µM after five minutes (54). Therefore, a concentration of 5 µM ZA was chosen for further study since all four cell lines exhibited a significant decrease in cell viability at seven days. MC3T3 (Figure 3.3), ST2, and MSC exhibited a greater decrease in cell viability when treated with 5 µM ZA compared to treatment with 5 Gy ($p < 0.0001$, $p = 0.001$, and $p = 0.070$, respectively), whereas the reverse was true for the F10 cells (Figure 3.4). There was no significant difference in cell viability between MC3T3 cells treated with 5 µM ZA or 10 Gy ($p = 0.83$), however combining radiation and ZA significantly decreased cell viability compared to either treatment alone ($p < 0.0001$). F10 cells showed a similar response, where treatment with 10Gy+ZA decreased cell viability more than ZA or 10Gy alone ($p < 0.0001$ and $p = 0.044$, respectively). The combination of radiation and ZA did not significantly effect cell viability compared to either treatment alone for the ST2 and MSC cell lines ($p > 0.05$).
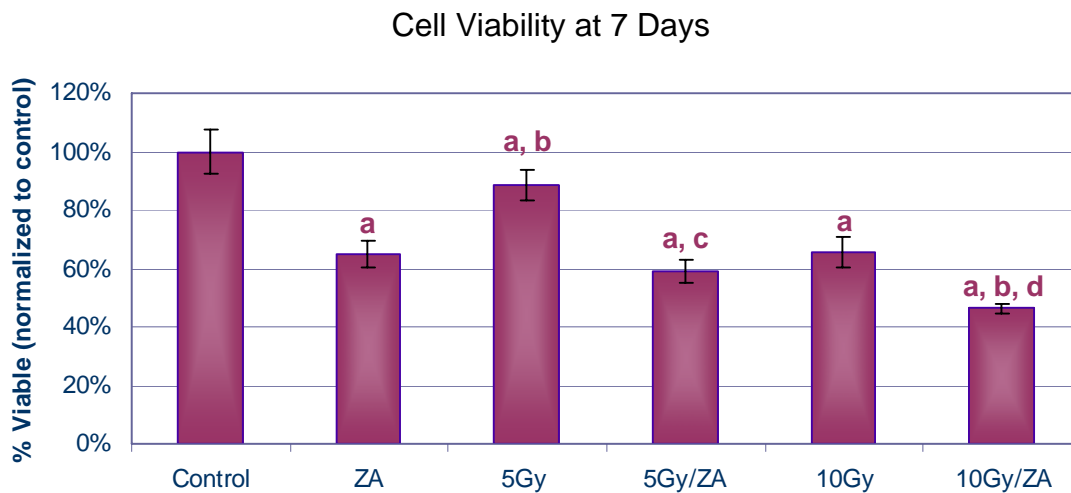

Figure 3.3: Effect of Radiation Therapy and ZA on MC3T3 Cell Viability Treatment with 5 µM ZA or 10 Gy lead to a similar decrease in cell viability and treatment with ZA+10Gy significantly decreased viability compared to either treatment alone. a = significant from control, b = significant from ZA, c = significant from 5Gy, d = significant from 10Gy Significance taken at $p < 0.05$)

Cell Viability at 7 Days

Figure 3.4: Effect of Radiation Therapy and ZA on F10 Cell Viability
Treatment with 5 μM ZA did not cause a significant decrease in cell viability compared to control. Treatment with ZA+10 Gy significantly decreased cell viability compared to either treatment alone. a = significant from control, b = significant from ZA, c = significant from 5 Gy d = significant from 10Gy Significance taken at $p < 0.05$.
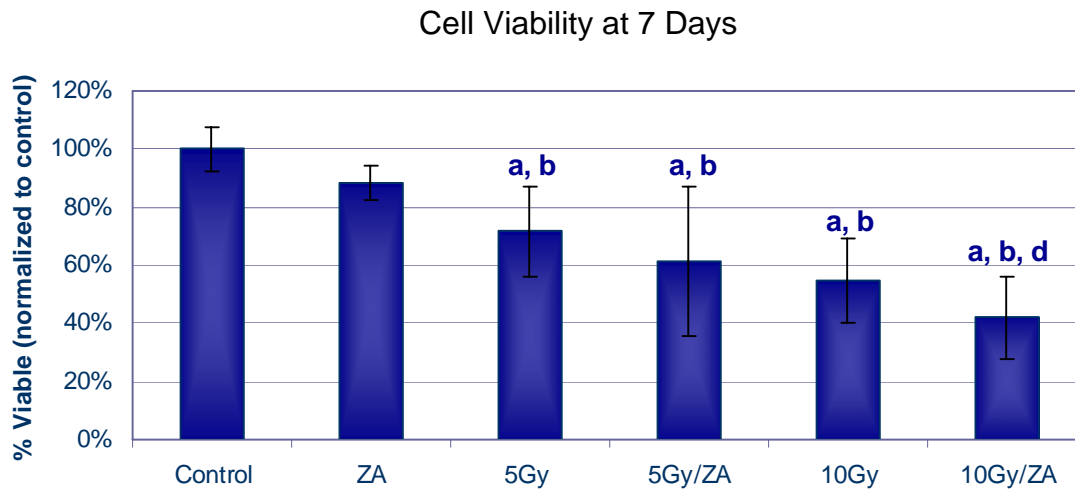
MC3T3 cells treated with 5 μM ZA or 10Gy+ZA displayed an increase in gene and protein expression of the pro-apoptotic Bax protein, however there did not appear to be a change in the gene expression of Bcl-2 (Figure 3.5). Cleaved caspase-3, which occurs downstream of Bax in the apoptosis cascade, was also increased in MC3T3 cells treated with 5 μM ZA or 10Gy+ZA compared to control ($p=0.029$ and $p=0.004$, respectively) (Figure 5.6). Treatment with 5 μM ZA or 10Gy+ZA also caused a significant increase in caspase-3 in ST2 ($p<0.0001$ and $p<0.0001$), MSC ($p=0.032$ and $p<0.0001$), and F10 ($p=0.024$ and $p=0.01$) cells compared to control.
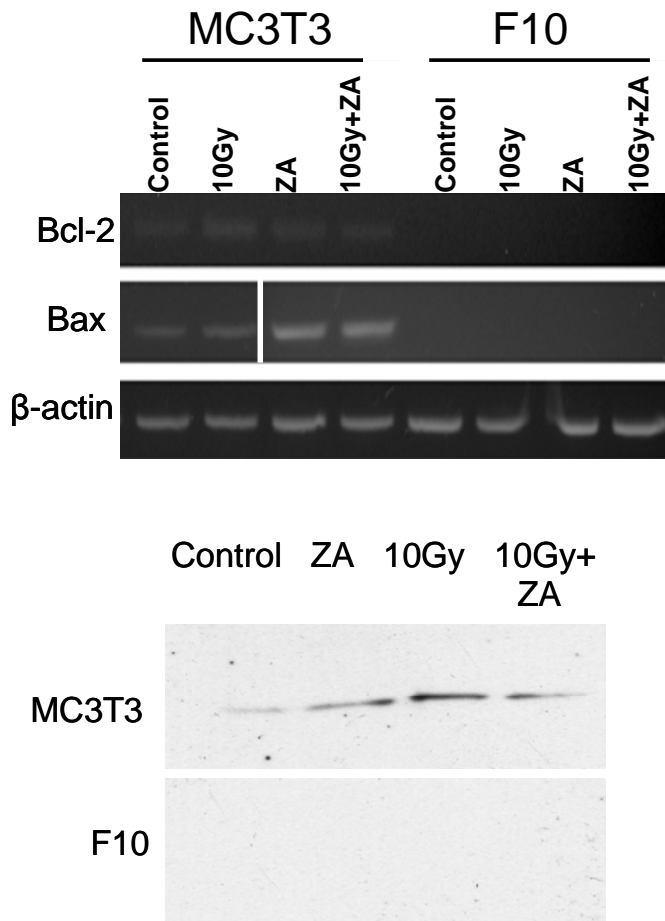
Figure 5.5: Detection of Early Apoptosis Markers

Top: RT-PCR gene expression of Bcl-2 (anti-apoptotic marker) and Bax (pro-apoptoic marker) in MC3T3 and F10 cells. Bcl-2 transcript expression remained relatively constant with respect to treatment in the MC3T3 cells, were Bax expression increased with exposure to ZA or 10Gy. Transcript expression of Bcl-2 and Bax was not detectable in the F10 cells.

Bottom: Western blot protein expression of Bax. Consistent with the RT-PCR data, Bax protein expression increased in the MC3T3 cells upon treatment with ZA or 10Gy. Protein expression of Bax was undetectable in the F10 cells.

Figure 3.6: Effect of Radiation and ZA on Apoptosis.
Treatment with 5 µM ZA lead to increased caspase in all four cell lines compared to control. F10 cells treated with 5 µM ZA and then irradiated with 10 Gy displayed increased caspase compared to control and treatment with 10 Gy alone. a = significant from control, b = significant from ZA, c = significant from 10Gy. Significance taken at $p<0.05$

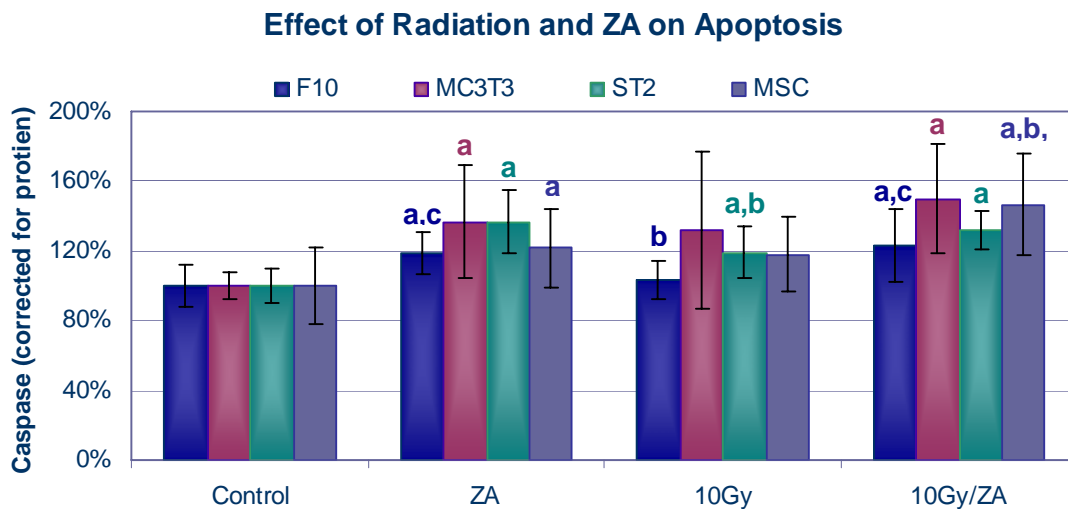F10 cells are known to have a high basal level expression of caspase-3; therefore to confirm that treatment with ZA and/or 10Gy induced apoptosis in these cells additional assays were performed. Immunohistochemistry confirmed that there was increased caspase localization to the nucleus in F10 cells treated with ZA, 10Gy, or 10Gy+ZA (Figure 3.6). It should be noted that the antibody used was for un-cleaved caspase-3, which explains the basal level of caspase staining seen in the control. In addition to caspase, Annexin V/ PI staining was performed to confirm apoptosis. These results indicate that treatment with 10Gy or 10Gy+ZA caused an increase in the number of cells expressing the phospholipid-like phosphatidyl-serine membrane protein on the outer surface of the cell membrane which binds Annexin V (Figure 3.7). Cells treated with 10Gy or 10Gy+ZA also showed increased PI binding, which occurs when PI is able to penetrate the cell membrane and bind to fragmented chromatin.
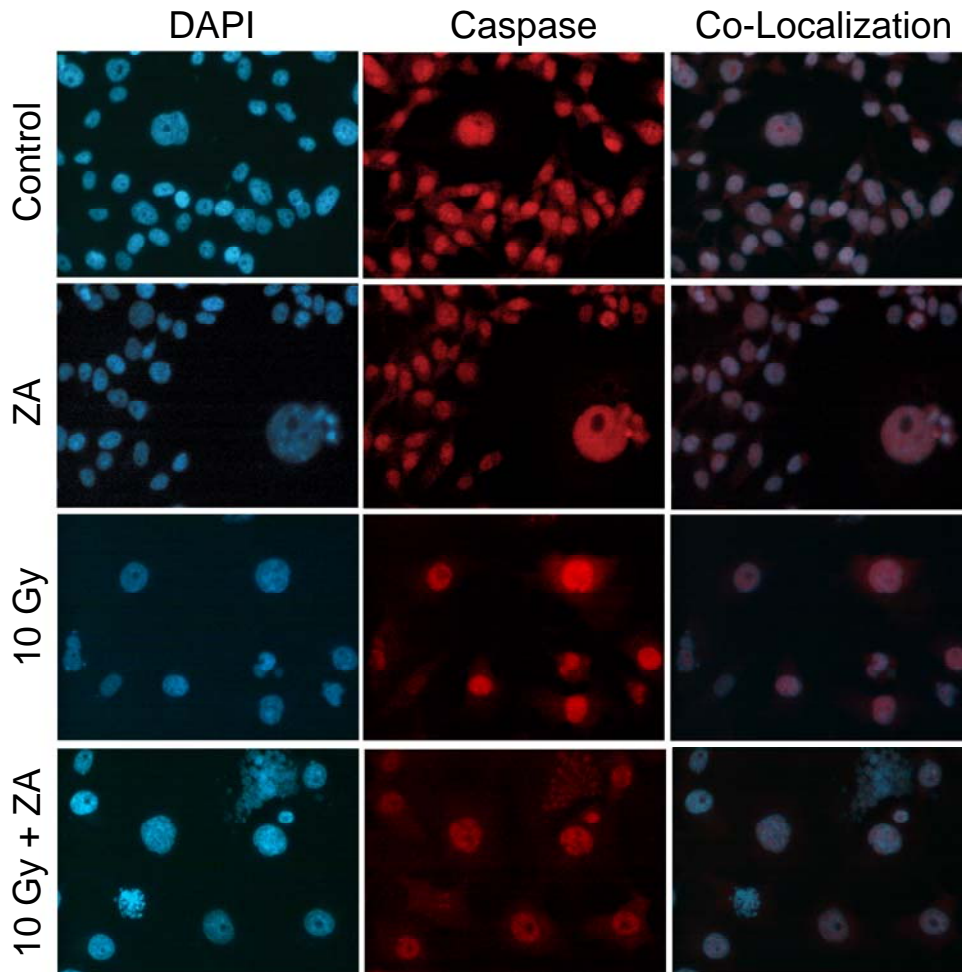
Figure 3.7: Qualitative Analysis of Apoptosis in F10 Breast Cancer Cells
Treatment with ZA and/or 10Gy resulted in increased caspase localization within nuclei that appear to be apoptotic, indicating that cells were undergoing the early stages of apoptosis. (2 days post-treatment)

26
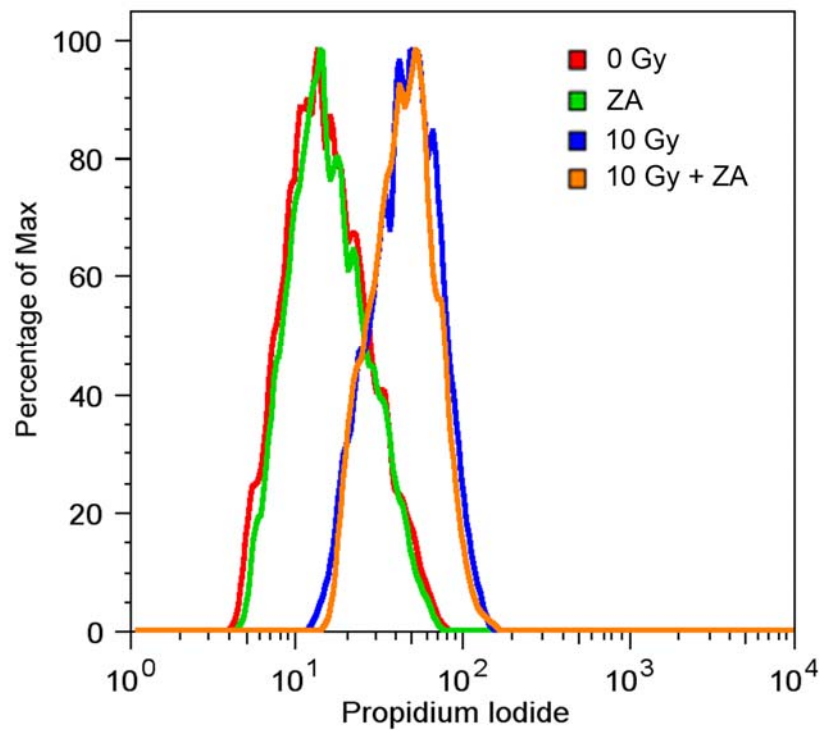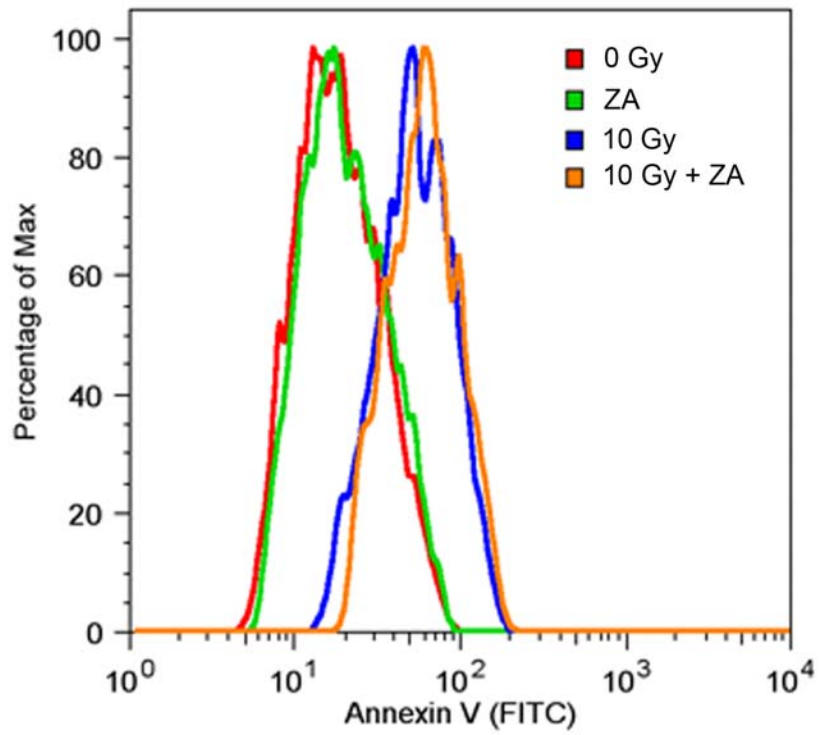
Figure 3.8: Detection of Annexin V and PI in F10 Cells Following Treatment
Two days following treatment with 10Gy or 10Gy+ZA F10 cells displayed an increase in Annexin V and PI staining compared to control and treatment with ZA alone, as measured by flow cytometry.

Effect of Radiation and Zoledronic Acid on the Cell Cycle

F10 cells treated with 5 µM ZA had a 13% increase in G_0/G_1 and a 23% decrease in G_2/M compared to control (p=0.008 and p=0.056), whereas treatment with 10 Gy led to a 20% decrease in G_0/G_1 and a 56% increase in G_2/M (p=0.001 and p=0.0001, respectively) (Figure 3.9A). 10Gy+ZA further increased G_2/M to 123% compared to control (p<0.0001). MC3T3 cells were most affected by treatment with ZA alone, which caused a 26% decrease in G_2/M and a 90% increase in S-phase compared to control (p<0.0001) (Figure 3.9B). ST2 cells were the only cells to exhibit an increase in G_2/M when treated with 5 µM ZA compared to control (27%, p=0.032). ST2 cells treated with 10Gy or 10Gy+ZA exhibited further increases in G_2/M (Figure 3.9C). MSC cells also had significant increases in G_2/M compared to control when treated with 10Gy or 10Gy+ZA (p<0.0001) (Figure 3.9D). Both the ST2 and MSC cells exhibited significant decreases in S-phase and G_0/G_1 when treated with 10 Gy or 10Gy+ZA (Figure 3.9 C and D).

A

B
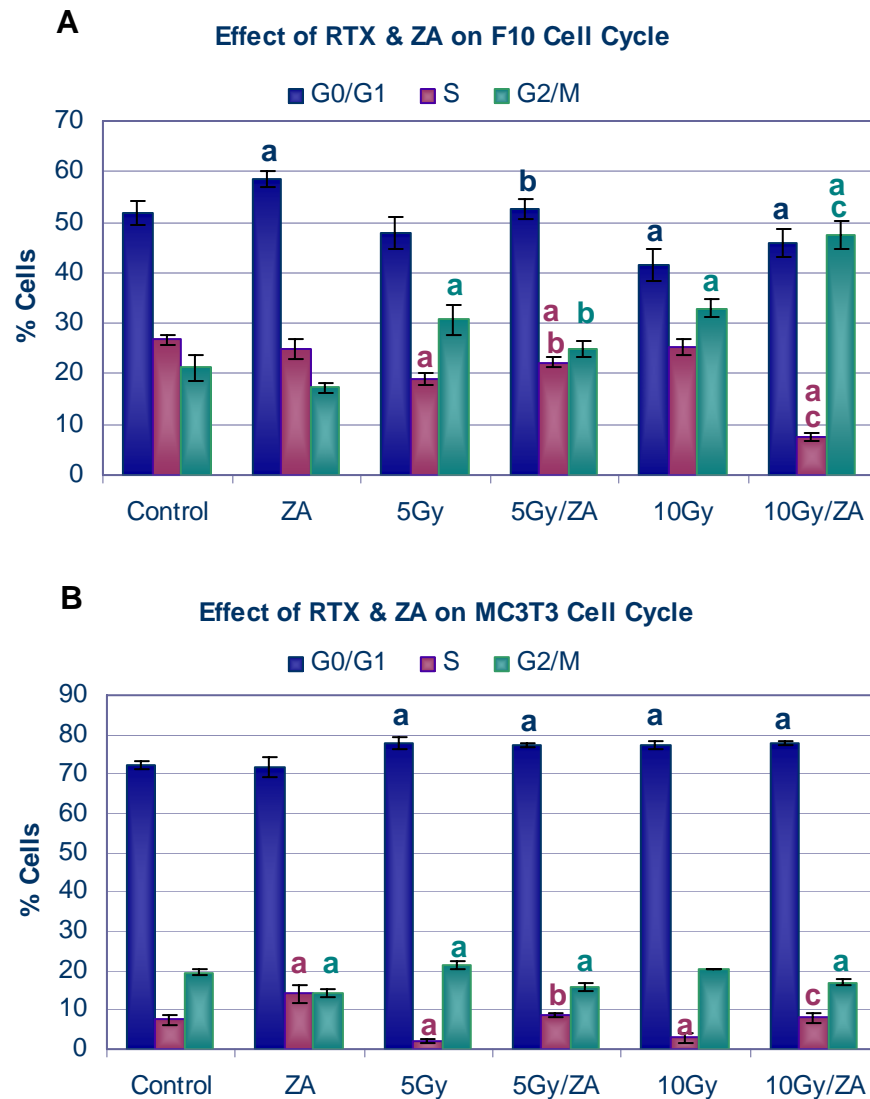
Figure 5.9A-D: Effect of Radiation Therapy and ZA on the Cell Cycle Treatment with ZA+10Gy caused increased G_2/M arrest in F10, ST2, and MSC cells compared to control, where MC3T3 cells displayed decreased G_2/M.
a = significant from control, b = significant from ZA, c = significant from 5Gy, d = significant from 10Gy. Significance taken at p<0.05

C

Effect of RTX & ZA on ST2 Cell Cycle

■ G0/G1   ■ S   ■ G2/M

D

Effect of RTX & ZA on MSC Cell Cycle

■ G0/G1   ■ S   ■ G2/M
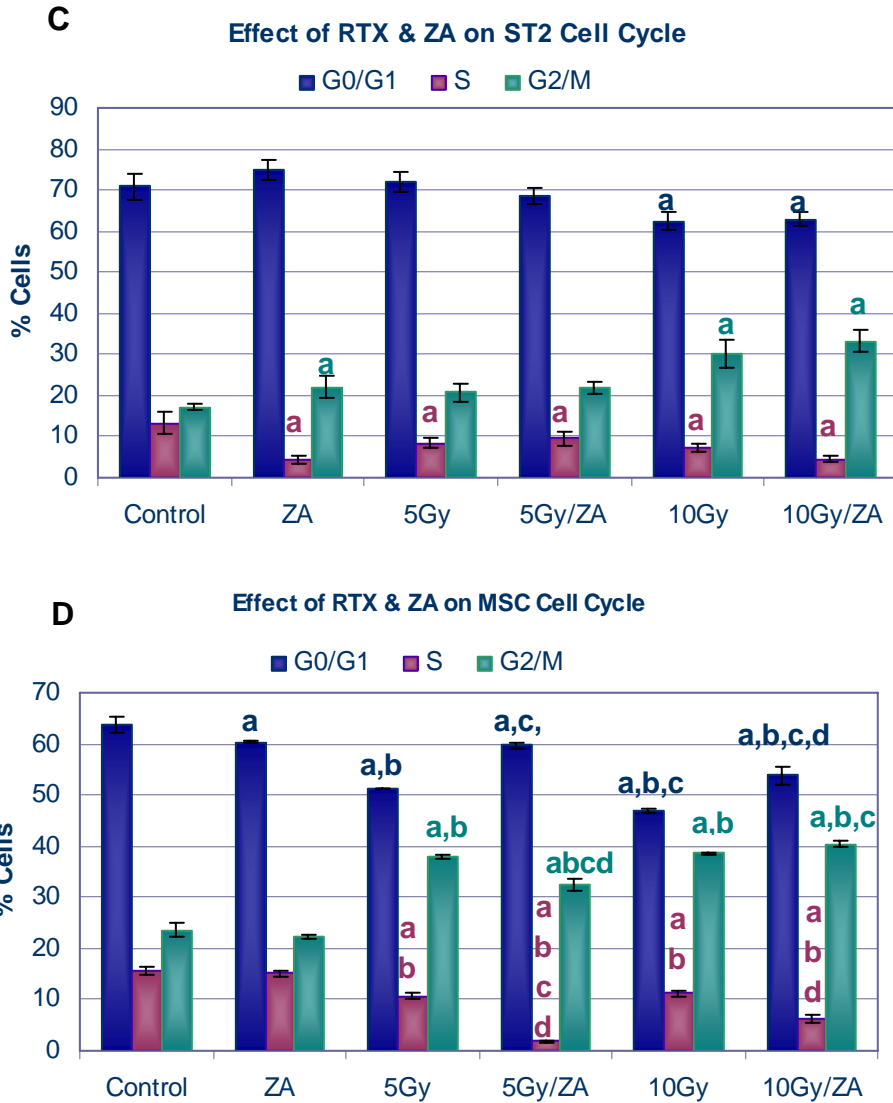
Figure 3.9A-D: Effect of Radiation Therapy and ZA on the Cell Cycle Treatment with ZA+10Gy caused increased G_2/M arrest in F10, ST2, and MSC cells compared to control, where MC3T3 cells displayed decreased G_2/M.
a = significant from control, b = significant from ZA, c = significant from 5Gy,
d = significant from 10Gy. Significance taken at $p < 0.05$

Effect of Radiation and Zoledronic Acid on Mineralization
Treatment with 10Gy decreased the amount of mineralization 32% in the MC3T3 cells compared to control ($p < 0.0001$) (Figure 3.10). 10Gy did not appear to affect the amount of mineralization in the MSC cells ($p = 0.315$). On the other hand, continuous exposure to 5 µM ZA resulted in significant cell death with a 93% decrease in mineralization in the MC3T3 cell line ($p < 0.0001$) (Figure 5.10). However, the MSC cell line displayed a 30% decrease in mineralization ($p < 0.0001$) compared to control. The combination of 10Gy+ZA resulted in increased cell death in the MC3T3 cells and decreased mineralization 69% in the MSC cell line compared to control ($p < 0.0001$).

29

It should be noted that the MSC cell line is not a homogeneous population of cells; rather it contains a mixture of cells found in the bone marrow. DAPI staining performed two days following treatment with ZA, 10Gy and 10Gy+ZA revealed that radiation appears to make the cell population more homogeneous (Figure 3.11). It is plausible that the surviving cells are bone marrow stromal cells that are more capable of mineralizing. This suggests that radiation may select more radioresistant osteoprogenitor cells. Further studies need to be conducted to determine the specific cell type remaining after radiation and whether treating primary bone marrow cultures with radiation may enhance the selection of bone marrow stromal cells.
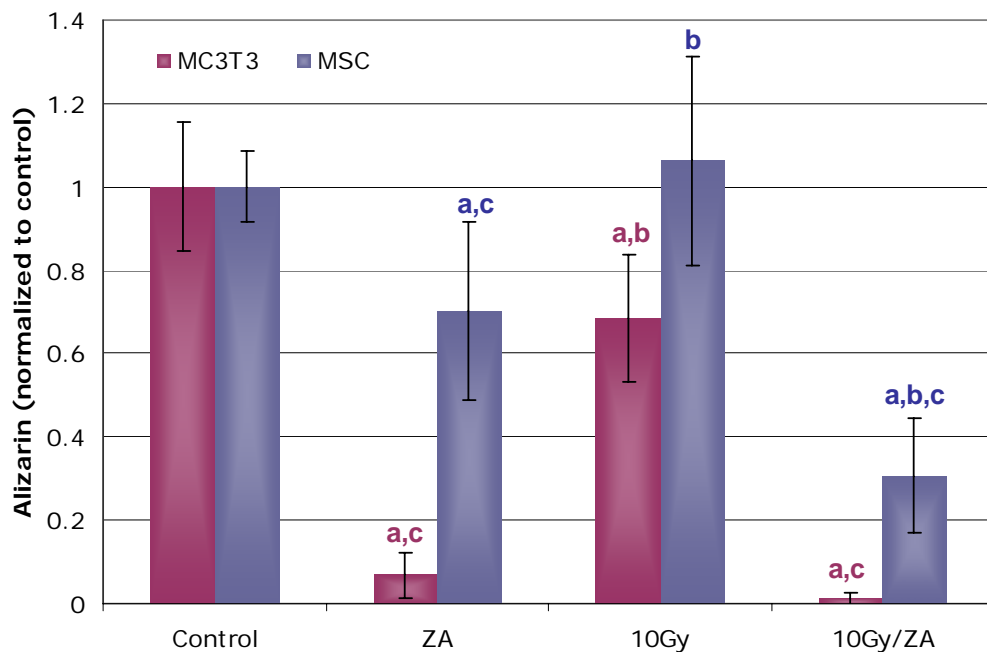
Figure 3.10: Effect of Radiation Therapy and ZA on Mineralization
Chronic treatment with 5 µM ZA for 21 days caused significant cell death in the MC3T3 cells, which corresponds to decreased mineralization. 10Gy appeared to cause an increase in MSC mineralization, however this was blunted with chronic exposure to ZA. a = significant from control, b = significant from ZA, c = significant from 10Gy Significance taken at $p < 0.05$
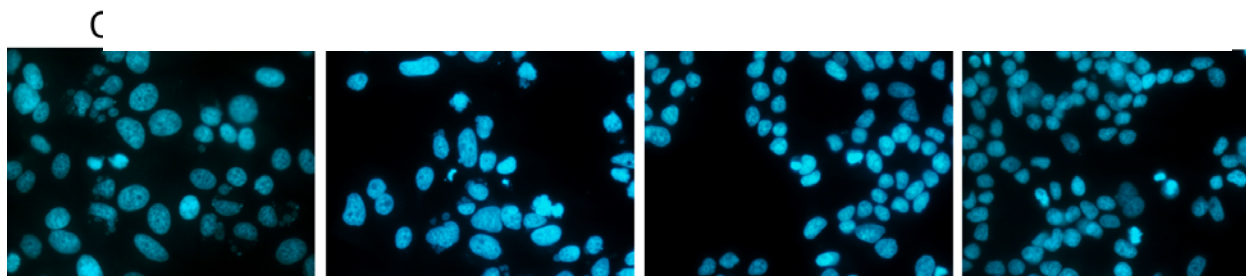
Figure 3.11: MSCs Stained with DAPI 2 Days Following Treatment
Note the diverse cell population in the control compared to the more uniform cell population seen after treatment with 10Gy. All images were taken at 40X.

Discussion

Radiation therapy and bisphosphonates are commonly used for the treatment of breast cancer bone metastases. In the present study, we have shown that the F10 human breast cancer line is more radiosensitive then MC3T3 (immortalized mouse osteoblast-like cells), ST2 (immortalized mouse stromal cells), and MSC (primary mouse marrow stromal cells). In addition, we have shown that F10 cells are less sensitive to zoledronic acid, with an IC_{50} nearly three times higher than that for MC3T3 cells and six times that of ST2 cells. In addition, F10 cells and MSCs displayed similar responses to treatment with 10Gy+ZA including, decreased cell viability, increased G_2/M arrest and increased caspase compared to treatment with 10Gy alone. This combined therapy also significantly decreased mineralization in the MSC cell line compared to radiation alone.

MC3T3 cells appeared to be very sensitive to continuous exposure to ZA, which lead to significant cell death. Unlike the F10 cells which displayed a significant increase in G_2/M arrest upon exposure to 10Gy+ZA, MC3T3 cells exhibited a significant decreased in G_2/M arrest and a significant increase in G_0/G_1. Even though treatment with 10Gy+ZA appears to cause apoptosis in both the F10 and MC3T3 cell lines, the mechanism through which this occurs appears to be different. These results of the present study suggest that zoledronic acid may have the potential to increase cell death in both tumor and bone cells when combined with radiation. Further studies are needed to determine whether similar effects can be achieved or enhanced by pre-treating cells with ZA prior to radiation and then rinsing the ZA our at various time points. The results of this set of experiments may provide a closer representation the cellular response to the combination of ZA and radiation *in vivo*.

Numerous *in-vitro* studies have been conducted to determine the effect of bisphosphonate and/or radiation on both tumor and bone cells (1, 12, 32, 43, 68, 85, 88). However, one of the major limitations of studying therapeutic responses in culture is being able to accurately model the *in vivo* exposure to these treatments. It has been calculated that the typical 4 mg dose of zoledronic acid used clinically in humans, results in a blood concentration around 1 to 2 µM (1, 13). However, we and others have found that it takes between 20 to 100 µM of zoledronic acid to kill 50% of the tumor cells (1, 32, 85). Although there is some debate regarding the concentration of bisphosphonates at the site of a lytic lesion, (800 µM at the osteoclast bone interface to <1 µM in the metastatic tumor burden near the bone)(75, 86), we have shown that a relatively low dose of ZA (5 µM) when combined with radiation is capable of inducing apoptosis in F10 cells beyond what is seen with radiation alone. These results strongly indicate that low concentrations of ZA are capable of sensitizing breast cancer cells to radiation therapy.

Bone cells, on the other hand, appear to be considerably more sensitive to bisphosphonates. Zoledronic acid [10^{-8} M] and pamidronate [10 µg/ml] have both been shown to increase proliferation and promote osteoblast differentiation (72, 88). In the current study however, we showed that slightly higher concentrations of zoledronic acid [5×10^{-8} M to 5×10^{-6} M] were capable of causing decreased viability and mineralization in both MC3T3 and MSC cell lines. Previous studies utilizing primary cell derived from human trabecular bone demonstrated that continuous exposure to 0.5 or 5 µM ZA caused a significant increase in mineralization compared to control following 35 days of treatment. viable cells displayed increased mineralization (68). However, they also report a significant decrease in cell viability of 30% to 40% compared to control after only three days of treatment. Measures of cell viability at 35 days were not reported; therefore it is unclear as to whether the cells in their culture continued to die or became resistant to the drug. Differences in mineralization seen in our study compared to Pan *et al* may be attributed to differences in osteoblast-like cell lines and their ability to differentiation when exposed to bisphosphonates. Additional studies using lower concentrations of ZA (<5×10^{-8} M) and shorter drug exposures (<24 hours) may represent more realistic *in-vivo* conditions and help determine whether or not bisphosphonates can directly stimulate increased mineralization.

Understanding the interactions between radiation, bisphosphonates and the tumor-bone microenvironment is important for optimizing clinical treatments and preventing negative side-effects. When evaluating chemical and pharmacologic agents as radiosensitizers, it is critical that the agent not only increases the sensitivity of the tumor to radiation, but it does not increase normal tissue sensitivity to

31

radiation. Through this study we have demonstrated that bone cells, including marrow stromal cells and osteoblast-like cells, are considerably more sensitive to zoledronic acid compared to tumor cells. In addition we have shown that pre-treating these cells with zoledronic acid prior to radiation therapy increases cell death. Therefore, even though zoledronic acid appears to have a synergistic affect with radiation on breast cancer cells the effect appears to be more pronounced for bone cells. Although zoledronic acid may not be a great radiosensitizer, do to its effects on both normal and tumor cells, it may still offer additional benefits for cancer patients. From a clinical perspective, it may be possible to decrease the radiation dose given to patients who are taking zoledronic acid and still maintain a therapeutic efficacy. Future investigations should focus on determining whether this effect can be obtained in culture as well as in pre-clinical models.

3.1. Key Research and Training Accomplishments
A. Research Accomplishments
- Purchase of a SCANCO μCT 40 scanner (SCANCO Medical, Switzerland)
  - Worked with programmers at SCANCO to develop custom programs to evaluate the bone microarchitecture of severely diseased bone
- Learned how to do thin section histology on bone and developed a sampling scheme to acquire an accurate representation of the interaction between tumor and bone
- Developed a detailed testing metric for evaluating the effects of antiresorptive and anabolic agents on tumor-burdened bone in a mouse model of breast cancer bone metastases
- Developed an *in vivo* microCT protocol for imaging nude mice serially

B. Training Accomplishments
- Shadowed Dr Kara Kort M.D., breast cancer surgeon at University Hospital. Sat in on patient consults, reviewed mammograms and MRI's, discussed treatment options for various types of breast cancer (ER+ versus ER-, age of the patient, family and health history, etc.).
- Attended monthly multidisciplinary breast cancer conferences with medical oncologists, radiation oncologists, and surgeons discussed complex breast cancer cases and treatment options.
- Attended the Carol M. Baldwin Breast Cancer Seminar
- Attended the Eighth and Valedictory Workshop on Bisphosphonates – From the Laboratory to the Patient; Davos, Switzerland (March 2006)
  - Submitted an abstract (Appendix 2) and presented a poster at the workshop
- Received advanced training on the SCANCO μCT 40 scanner at SCANCO Medical; Basserdorf, Switzerland
- Attended the VI International Meeting on Cancer Induced Bone Disease; San Antonio, TX
  - Submitted an abstract (Appendix 3) and presented a poster at the meeting
  - Received a travel grant based on my abstract
- Gave a seminar at SUNY Upstate Medical University sponsored by the department of Neuroscience and Physiology entitled *Adjuvant Therapy with Zoledronic Acid and PTH: Safe and Effective for the Treatment of Osteolytic Bone Metastases in the Mouse*; October 19, 2006
- Presented the following oral presentation: "Zoledronic acid restores bone microarchitecture and mechanical strength to tumor-burdened bones following radiation therapy", S.A. Arrington, E.R. Fisher, J.A. Gasser, G. Willick, K.A. Mann, M.J. Allen, at SUNY Upstate Medical University, Department of Orthopaedics, Alumni Day June 2007.

- Presented the following poster: "Zoledronic acid and PTH increase bone mass and mechanical strength following radiation theray for osteolytic bone metastases" S.A. Arrington, J.E. Schoonmaker, K.A. Mann, T. Sledz, G. Willick, T.A. Damron, M.J. Allen, SUNY Upstate, at The Department of Microbiology and Immunology, Human Disease Models: SCID Mice, Stem Cells, and Viral Pathogenesis symposium, May 2007.

- Attended the 29th Annual meeting of the American Society for Bone and Mineral Research, Honolulu, HI, September 2007
  - Submitted an abstract (Appendix 4) and presented a poster at the meeting

4. Reportable Outcomes
4.1: Peer Reviewed Publications

1. Arrington, S.A.; Damron, T.A; Mann, K.A.; and Allen, M.J. (2007). Concurrent Administration of Zoledronic Acid and Irradiation Leads to Improved Bone Density, Biomechanical Strength, and Microarchitecture in a Mouse Model of Tumor-Induced Osteolysis. *Journal of Surgical Oncology* (Accepted November 2007)

2. Arrington, S.A.; Schoonmaker, J.E.; Damron, T.A.; Mann, K.A.; Allen, M.J. (2006). Temporal changes in bone mass and mechanical properties in a murine model of tumor osteolysis. BONE 38, 359-367.

4.2: Abstracts and Poster Presentations
1. S. A. Arrington, B. S. Margulies, E. R. Fisher, M. J. Allen. (September 2007) *In Vitro* Effects of Zoledronic Acid Alone or in Combination with Radiation Therapy on Cells of the Metastatic Bone Environment. Poster presented at the 29th Annual American Society for Bone and Mineral Research Meeting, Honolulu, Hawaii.

2. Arrington, S.A.; Schoonmaker, J.E.; Mann, K.A.; Damron, T.A.; Sledz, T.; Willick, G.; and Allen, M.J. (May 2007) Zoledronic acid and PTH increase bone mass and mechanical strength following radiation therapy for osteolytic bone metastases. Poster presented at The Department of Microbiology and Immunology SUNY Upstate Medical University, Human Disease Models: SCID Mice, Stem Cells, and Viral Pathogenesis symposium.

3. Arrington, S.A.; Schoonmaker, J.E.; Mann, K.A.; Damron, T.A.; Sledz, T.; Willick, G.; and Allen, M.J. (2006) Zoledronic acid and PTH increase bone mass and mechanical strength following radiation therapy for osteolytic bone metastases • ABSTRACT BONE 38, Supplement 1, S43 Poster presented at the Eighth and Valedictory Workshop on Bisphosphonates: From the laboratory to the patient. Davos, Switzerland.

4. Arrington, S.A.; Fisher, E.R.; Gasser, J.A.; Willick, G.; Allen, M.J. (December 2006) Zoledronic Acid and PTH Increase Survival and Quality of Life Following Radiation Therapy for Osteolytic Bone Metastases. Poster Presented at VI International Meeting on Cancer Induced Bone Disease. San Antonio, Texas.

4.3: Oral Presentations

1. Arrington, S.A. (Dec. 12, 2007) Effect of Anabolic and Antiresorptive Therapies on Tumor Osteolysis. Thesis defense seminar presented at SUNY Upstate Medical University.

2. Arrington, S.A., Fisher, E.R.; Gasser, J.E.; Willick, G.E.; Mann, K.A.; Allen, M.J. (2007) Zoledronic acid restores bone microarchitecture and mechanical strength to tumor-burdened bones following radiation therapy. Oral presentation presented at SUNY Upstate Medical University, Department of Orthopedic Surgery, Alumni Day, June 2007

4.4: Degrees and Employment
1. Received a Ph.D. in Physiology from SUNY Upstate Medical University December 14, 2007

2. Received an appointment in the departments of Biology and Chemistry at Shepherd University, Shepherdstown, West Virginia were I will also work to develop advanced level courses in cancer biology.

5.0: Conclusions

Breast cancer metastasis to bone disrupts the physiological process of bone remodeling, resulting in increased bone resorption. Prior to the discovery of bisphosphonates, treatment for these patients was limited to systemic hormonal or chemotherapy aimed at killing metastatic tumor cells, and localized radiation therapy to palliate bone pain. Although these treatments reduce tumor burden and bone pain, they do not reduce the risk or incidence of pathological fractures. In addition, we have learned that both tamoxifen and aromatase inhibitors, widely used in the management of estrogen receptor positive tumors, affect bone density and strength. Therefore, it is vital that we increase our understanding of the mechanisms underlying bone mineralization and trabecular bone formation and how these properties correlate to biomechanical strength. Only then can we develop and optimize therapies to treat cancer-induced bone disease.

5.1: Improved Pre-Clinical Model of Bone Metastasis
Pre-clinical animal models of bone metastasis are commonly used to study the process of metastatic disease as well as therapeutic interventions used to prevent and control the spread of metastatic cancer cells (44, 50, 51, 67, 91). In this dissertation, we have developed and validated a mouse model in which the effects of an established lytic bone lesion in bone can be assessed. The goal of this model was to closely mirror the clinical setting with respect to cell type, location of the metastasis, modalities used to monitor disease progression, and therapies used to treat bone metastases. In addition, we also wanted to assess bone strength as an indicator of fracture risk. Although several animal models exist, none of them fully recapitulate this clinical approach. The benefit to developing a model system that utilizes similar techniques to those used clinically is that these methods should be easier to translate into clinical use in humans.

Since pathological fracture is a devastating complication of bone metastasis, we consider biomechanical strength to be the most important outcome measure. Although a diseased bone may have improved bone density and/or microarchitecture, bone strength does not necessarily increase. Therefore, when evaluating the efficacy of therapies it is important to determine the effect they have on functional bone strength. In this dissertation, we have validated a new model of whole-limb torsional testing. Unlike traditional torsional testing, where both ends of the bone are potted, we developed a method where the proximal end of the femur and the distal end of the tibia are potted, allowing rotation to occur through the intact knee joint. In this test method, fractures occur through the diseased area of the bone. We have demonstrated that although the strength of normal bones may be underestimated, since the ligaments may sometimes be weaker than the bone, significant differences in bone strength can be measured between tumor-burdened bones, treated tumor-burdened bones, and normal bones.

X-rays, DEXA, and CT are all clinically available techniques that can be used to monitor the progression of tumor osteolysis. Currently, osteolytic lesions are monitored by X-rays and a weighted scoring system has been developed to predict fracture risk (64). A similar system was developed by Weber *et al* for scoring osteolytic lesions in a mouse model of tumor-induced osteolysis (90). We adapted this scoring system and correlated it to biomechanical strength. Results from our studies showed that lysis ratings could explain 73% of the variation in torque at failure.

DEXA scans, on the other hand, are commonly used to predict bone strength in patients with osteoporosis. As this is a clinically obtainable measure, we sought to determine whether or not bone mineral density measures obtained from DEXA scans could be used to predict the strength of tumor-burdened bones. Regression analysis indicated that BMD could only explain 41% of the variation in torque at failure (2). Measurements of BMD do not appear to be a better indicator of biomechanical strength in tumor-burdened bone and therefore are not recommended for clinical assessment of biomechanical strength in tumor-burdened bones.

The development of μCT scanners has greatly enhanced our ability to study the effects of disease and therapies on bone microarchitecture. It is well known that trabecular bone undergoes remodeling in response to mechanical forces (61), and is significantly affected in diseases where the balance between bone resorption and bone apposition is disrupted. We hypothesized that loss of trabecular bone causes a

34

significant decrease in biomechanical strength. We were able to demonstrate that although bones treated with radiation therapy exhibited significantly higher bone mineral density and total bone volume compared to untreated bones, they were not significantly stronger (see Chapter III). However, both the untreated and irradiated tumor-burdened bones had significantly lower trabecular bone compared to normal. These results suggest that therapies that can preserve or restore trabecular bone may be effective at restoring biomechanical strength.

Although the studies conducted in this dissertation were not amenable for direct analysis between bone microarchitecture and strength, our laboratory is currently developing a methodology for determining bone strength using µCT scans and computational techniques (59). Utilizing our murine model of tumor-induced osteolysis to obtain a wide-range of lesion sizes, we compared the accuracy of radiographic scores, BMD measurements obtained from DEXA, and direct CT voxel-based finite element analysis (CT/FEA) to predict the bone strength. Direct axial compression of the distal femur was performed to assess biomechanical strength that could also be modeled using FEA. Based on these tests we were able to demonstrate that specimen-specific CT/FEA resulted in the highest prediction of bone strength (r^2=0.91). Future studies will focus on predicting the strength of tumor-bearing bones treated with various therapies.

Further development of this imaging modality has powerful clinical potential. Currently clinicians rely on X-rays and Mirels scoring system to predict risk of pathological fracture. However, this method has low specificity, with approximately two-thirds of patients undergoing unnecessary internal fixation when Mirles criteria are strictly applied (20, 64). Presently, the long scan times, dose of radiation, and large model size prevent direct application CT/FEA for predicting bone strength in human patients. However with advancements in computer technology, this approach may provide clinicians with a more reliable modality for predicting fracture risk in the near future.

5.2: Zoledronic Acid and Bone Metastases
Zoledronic acid (ZA) is the most potent bisphosphonate approved for use in patients with bone metastases and has been shown to significantly decrease skeletal complications in clinical trials. The goal of the present work was to determine the effects that ZA had on the progression of tumor-induced osteolysis, bone microarchitecture and biomechanical strength when combined with radiation therapy. We were able to demonstrate through serial radiographs and DEXA scans that tumor-bearing bones treated with radiation therapy and ZA were able to maintain bone mineral density that was not significantly different from normal from the start of treatment to the end of the study. This is in contrast to bones that were only treated with radiation therapy, which showed a significant decrease in bone mineral density compared to normal bones within three weeks following therapy. This change in mineralization was also observed on radiographs. However, it should be noted that in a pilot study, where mice with established lesions were treated with ZA alone, tumor osteolysis was not prevented and there was not a significant difference between untreated and ZA treated tumor-bearing bones with respect to total bone volume. Therefore it is not recommended that ZA be used as a stand-alone therapy for the treatment of an established bone metastasis.

5.3: The Role of Anabolic Therapy
Anabolic therapy has been used successfully in the treatment of osteoporosis (21). Although the use of anabolics in treating cancer related disease is contentious, we sought to determine whether additional benefits in bone microarchitecture and strength could be obtained through a combined anti-resorptive – anabolic therapy. Currently, there is no evidence that bisphosphonates can make bone. Relative increases observed in bone mineral density (compared to normal bone) in both clinical and pre-clinical studies, can be attributed to decreased resorption and filling in of the remodeling space. Therefore, it may be advantageous to include an anabolic agent, which has the capacity to form new bone.

Parathyroid hormone (PTH) plays a critical role in calcium homeostasis through its actions on the bone, kidney, and intestine (10). Physiologically, when Ca^{2+} serum levels decrease, parathyroid cells increase the secretion of PTH which leads to increased bone resorption. PTH stimulates osteoclastic bone resorption by binding to its receptor (PTH1R) located on mature osteoblasts. This action causes osteoblasts to produce receptor activator of nuclear factor-κB ligand (RANKL) which binds to its receptor

(RANK) on osteoclastic precursors. This leads to the formation of mature osteoclasts. Under normal conditions, the rate of bone resorption is balanced by bone formation. However, chronic exposure to high levels of PTH can disrupt this balance and cause net bone loss. Conversely, intermittent exposure to low doses of PTH (too small to affect serum calcium concentrations) promotes bone formation and can increase bone mineral density (46). Although the mechanisms for this anabolic effect are not fully understood, it is known that PTH reduces the prevalence of apoptosis in osteoprogenitor cells and osteoblasts (46) and has been found to activate bone lining cells into active osteoblasts (25). Based on the anabolic affects of intermittent PTH, recombinant human parathyroid hormone (PTH 1-34, Forteo) was developed by Eli Lilly and Company for the treatment of osteoporosis (21).

When treating osteolytic bone diseases, such as osteoporosis or metastatic breast cancer, the goal of therapy is to preserve the bone and prevent pathological fracture. For cases of severe osteolysis it may be beneficial to combine the anti-resorptive properties of bisphosphonates with the anabolic properties of intermittent PTH. Several studies have been conducted both clinically and in animal models to determine the effect of combining hPTH (1-34) with a bisphosphonate (18, 35, 62). However, the results of these studies have been inconclusive, with some stating that the effect of PTH is blunted due to decreased bone resorption caused by the bisphosphonates, while others report that its actions are unaffected. The goal of the current study was to determine whether PTH was capable of improving bone microarchitecture and biomechanical strength, when combined with ZA and radiation therapy.

Using our model of tumor-induced osteolysis, we have demonstrated that treatment with hPTH $(1-34)NH_2$ and ZA as adjuncts to radiation therapy was effective in of significantly increasing bone mineral density, total bone volume, and trabecular thickness compared to normal bones. No statistical difference was found between normal, radiation+ZA, and radiation+ZA+PTH bones with respect to mechanical strength or fractional trabecular bone volume. These results support our hypothesis that mechanical strength is closely linked with trabecular bone, rather than total bone volume. However, it should also be noted that on average, tumor-burdened bones treated with radiation+ZA+PTH required less energy to reach failure compared to radiation+ZA and normal bones. This may be due to(58, 65, 78) differences in mineralization which would affect the material properties of the bone. Although PTH may not be the ideal anabolic agent for the treatment of bone metastases, our results demonstrate that such agents may provide an effective mechanism to increase functional bone strength. Continued research investigating the efficacy of other potential anabolics, such as those that directly stimulate bone morphogenic proteins (BMPs) (15) or prostaglandin EP4 antagonist (58, 65, 78), is warranted.

5.4: Cellular Sensitivity to Radiation and Zoledronic Acid

The role of bisphosphonates as anti-tumor agents has been studied by various laboratories in both *in-vitro* and *in-vivo* systems. We, along with others, have shown that a concentration of 20 to 100 μM of bisphosphonate is required to induce a 50% decrease in cell viability (1, 32, 43, 77). Although the exact concentration of bisphosphonate that a tumor cell would be exposed to is unknown, clinical studies report a blood concentration around 1 to 2 μM based on a 4mg dose of zoledronic acid (1, 13). However, recent studies have shown that after four years of treatment with ZA (4 mg/month), the bone level would be around 70 nmol/gram of bone [ref]. In the event that bone is resorbed, it is not unreasonable that tumor cells could be exposed to toxic levels of ZA. Studies on osteonecrosis of the jaw due with respect to bisphosphonate have shown that a toxic effect is observed in epithelial cells at 1nmol/ml (71). Therefore, it may be possible for bisphosphonates to induce cell death in tumor cells at sites near active bone resorption.

The interaction between bisphosphonates and osteoclasts is well known, however the effect of bisphosphonates on other bone cells, including osteoblasts and marrow stromal cells, are not fully understood. Recent studies have shown that osteoblasts appear to be more sensitive to bisphosphonates then tumor cells, showing increased proliferation and mineralization at a very low concentrations (10^{-8} M ZA). However, slightly higher concentrations around 0.5 to 5 μM appear to cause increased cell death (see section 3.2) (68). Since osteoblasts are attracted to areas of active bone remodeling, it is probable that these cells could be exposed to a reasonable concentration of bisphosphonate; and therefore increase mineralization in the area around newly resorbed bone.

36

In addition to the direct effects of bisphosphonates on cell death, it has been proposed that they may also sensitize cells to radiation (1). In this dissertation we have shown that zoledronic acid, at a concentration of 5 µM, combined with 10 Gy radiation was capable of decreasing cell viability, increasing caspase activity, and increasing G_2/M arrest compared to radiation alone. Therefore, administering zoledronic acid prior to radiation therapy may enhance tumor cell sensitivity to radiation. Further studies are warranted to determine whether this is an additive or synergistic effect. If we can demonstrate that tumor-burdened bones treated with zoledronic acid and lower doses of radiation are still capable of regaining near normal bone microarchitecture and biomechanical strength, this would have a huge impact on the clinical treatment of human patients by decreasing the adverse side effects of high doses of radiation.

5.5: Conclusions and Future Directions

Taken together, the results of our *in-vivo* studies have shown that our model provides a relevant platform for investigating therapeutic treatments for osteolytic bone metastases. Clinically relevant screening techniques and therapies are easily applied to this model. In addition, we are able to evaluate functional outcomes, such as biomechanical strength, which are not easily obtained through clinical studies. Adapting the techniques used in this model system, more robust screening methods can be developed and rapidly translated to the clinical setting. We have shown that trabecular architecture appears to play a critical role in bone strength, therefore if we can correlate key trabecular structures with biomechanical strength, physicians may be able to use CT scans to more accurately predict impending fractures in patients with bone metastases.

The development of *in-vivo* µCT scanners also adds an exciting dimension to the study of bone metastases. At the start of this dissertation *ex-vivo* specimen µCT scanners were a novel method for studying bone microarchitecture; now three years later, they are an essential part of any bone study. Although these systems allowed us to evaluate the effects of disease and treatments on bone at the end of a study, they did not allow for study of disease/treatment progression. Today, *in-vivo* µCT scanners allow for statistically more robust experiments with fewer animals due to the ability to perform paired analyses with decreased variability between groups. In this dissertation we have developed at protocol for using an *in-vivo* scanner to follow the progression of tumor induced osteolysis in our mouse model. Future studies will continue to build on this protocol and these should allow us to determine the strength of tumor-burdened bones at the time of treatment and throughout the course of the study by correlating serial CT data with biomechanical analysis. However, *ex-vivo* µCT still provides a better platform for detailed analyses of microarchitecture.

Although the studies conducted in this dissertation focused on a single breast cancer cell line, it should be noted that this model is amenable to studying other primary tumors that metastasize to bone, including prostate and renal cancer, as well as primary bone tumors including osteosarcoma and Ewing's sarcoma (60). The outcome measures utilized in our studies, including X-rays, DEXA scans, µCT, and biomechanical testing, are all applicable to studying these various types of tumors. In addition, advances in molecular biology that aid in the development of cell lines that stably express fluorescent and bioluminescent genes, such as GFP and luciferase, will allow for the quantification of tumor burden over time and in response to therapies. Taken together, we have developed and validated an *in-vivo* model system that can be utilized to study the physiology of tumor-induced bone disease, to establish efficacy of new therapies for treating bone metastases, and to develop and validate new screening modalities to assess fracture risk that can be easily translated to the clinical setting.

37

6. References

1.   Algur, E., Macklis, R. M., and Hafeli, U. O. Synergistic cytotoxic effects of zoledronic acid and radiation in human prostate cancer and myeloma cell lines. Int J Radiat Oncol Biol Phys 61*:*535-42; 2005.

2.   Arrington, S. A., Schoonmaker, J. E., Damron, T. A., Mann, K. A., and Allen, M. J. Temporal changes in bone mass and mechanical properties in a murine model of tumor osteolysis. Bone 38*:*359-67; 2006.

3.   Bell, G. H., Dunbar, O., Beck, J. S., and Gibb, A. Variations in strength of vertebrae with age and their relation to osteoporosis. Calcif Tissue Res 1*:*75-86; 1967.

4.   Bevill, G., Eswaran, S. K., Gupta, A., Papadopoulos, P., and Keaveny, T. M. Influence of bone volume fraction and architecture on computed large-deformation failure mechanisms in human trabecular bone. Bone 39*:*1218-25; 2006.

5.   Body, J. J. Bisphosphonates for malignancy-related bone disease: current status, future developments. Support Care Cancer 14*:*408-18; 2006.

6.   Body, J. J., Bartl, R., Burckhardt, P., Delmas, P. D., Diel, I. J., Fleisch, H., Kanis, J. A., Kyle, R. A., Mundy, G. R., Paterson, A. H., and Rubens, R. D. Current use of bisphosphonates in oncology. International Bone and Cancer Study Group. J Clin Oncol 16*:*3890-9; 1998.

7.   Body, J. J., Diel, I. J., Lichinitzer, M., Lazarev, A., Pecherstorfer, M., Bell, R., Tripathy, D., and Bergstrom, B. Oral ibandronate reduces the risk of skeletal complications in breast cancer patients with metastatic bone disease: results from two randomised, placebo-controlled phase III studies. Br J Cancer 90*:*1133-7; 2004.

8.   Boone, J. M., Velazquez, O., and Cherry, S. R. Small-animal X-ray dose from micro-CT. Mol Imaging 3*:*149-58; 2004.

9.   Brouwers, J. E., van Rietbergen, B., and Huiskes, R. No effects of in vivo micro-CT radiation on structural parameters and bone marrow cells in proximal tibia of wistar rats detected after eight weekly scans. J Orthop Res 25*:*1325-32; 2007.

10.   Brown, E. M., and Juppner, H. Parathyroid Hormone: Synthesis, Secretion, and Action. In*:* S. Christakos and M. F. Holick (eds.), Primer on the Metabolic Bone Diseases and Disorders of Mineral Metabolism, pp. 90-98. Washington D.C.: American Society for Bone and Mineral Research; 2006.

11.   Cefalu, C. A. Is bone mineral density predictive of fracture risk reduction? Curr Med Res Opin 20*:*341-9; 2004.

12.   Chen, M. F., Lin, C. T., Chen, W. C., Yang, C. T., Chen, C. C., Liao, S. K., Liu, J. M., Lu, C. H., and Lee, K. D. The sensitivity of human mesenchymal stem cells to ionizing radiation. Int J Radiat Oncol Biol Phys 66*:*244-53; 2006.

13.   Chen, T., Berenson, J., Vescio, R., Swift, R., Gilchick, A., Goodin, S., LoRusso, P., Ma, P., Ravera, C., Deckert, F., Schran, H., Seaman, J., and Skerjanec, A. Pharmacokinetics and pharmacodynamics of zoledronic acid in cancer patients with bone metastases. J Clin Pharmacol 42*:*1228-36; 2002.

14.   Clemons, M., Dranitsaris, G., Cole, D., and Gainford, M. C. Too much, too little, too late to start again? Assessing the efficacy of bisphosphonates in patients with bone metastases from breast cancer. Oncologist 11*:*227-33; 2006.

15.   Clohisy, D. Cellular mechanisms of osteolysis. Journal of Bone & Joint Surgery - American Volume 85-A Suppl 1*:*S4-6; 2003.

16.   Clohisy, D. R., Palkert, D., Ramnaraine, M. L., Pekurovsky, I., and Oursler, M. J. Human breast cancer induces osteoclast activation and increases the number of osteoclasts at sites of tumor osteolysis. J Orthop Res 14:396-402; 1996.

17.   Coran, A. G., Banks, H. H., Aliapoulios, M. A., and Wilson, R. E. The management of pathologic fractures in patients with metastatic carcinoma of the breast. Surg Gynecol Obstet 127:1225-30; 1968.

18.   Cosman, F., Nieves, J., Woelfert, L., Shen, V., and Lindsay, R. Alendronate does not block the anabolic effect of PTH in postmenopausal osteoporotic women. J Bone Miner Res 13:1051-5; 1998.

19.   Croucher, P., Jagdev, S., and Coleman, R. The anti-tumor potential of zoledronic acid. Breast 12 Suppl 2:S30-6; 2003.

20.   Damron, T. A., and Ward, W. G. Risk of pathologic fracture: assessment. Clin Orthop Relat Res:S208-11; 2003.

21.   Deal, C., and Gideon, J. Recombinant human PTH 1-34 (Forteo): an anabolic drug for osteoporosis. Cleve Clin J Med 70:585-6, 589-90, 592-4 passim; 2003.

22.   Delmas, P. D., Vergnaud, P., Arlot, M. E., Pastoureau, P., Meunier, P. J., and Nilssen, M. H. The anabolic effect of human PTH (1-34) on bone formation is blunted when bone resorption is inhibited by the bisphosphonate tiludronate--is activated resorption a prerequisite for the in vivo effect of PTH on formation in a remodeling system? Bone 16:603-10; 1995.

23.   Diel, I. J., Solomayer, E. F., and Bastert, G. Treatment of metastatic bone disease in breast cancer: bisphosphonates. Clin Breast Cancer 1:43-51; 2000.

24.   Divittorio, G., Jackson, K. L., Chindalore, V. L., Welker, W., and Walker, J. B. Examining the relationship between bone mineral density and fracture risk reduction during pharmacologic treatment of osteoporosis. Pharmacotherapy 26:104-14; 2006.

25.   Dobnig, H., and Turner, R. T. Evidence that intermittent treatment with parathyroid hormone increases bone formation in adult rats by activation of bone lining cells. Endocrinology 136:3632-8; 1995.

26.   Elte, J. W., Bijvoet, O. L., Cleton, F. J., van Oosterom, A. T., and Sleeboom, H. P. Osteolytic bone metastases in breast carcinoma pathogenesis, morbidity and bisphosphonate treatment. Eur J Cancer Clin Oncol 22:493-500; 1986.

27.   Erben, R. G. Embedding of bone samples in methylmethacrylate: an improved method suitable for bone histomorphometry, histochemistry, and immunohistochemistry. J Histochem Cytochem 45:307-13; 1997.

28.   Faulkner, K. G. Bone matters: are density increases necessary to reduce fracture risk? Journal of Bone & Mineral Research 15:183-7; 2000.

29.   Fitts, W. T. J., Roberts, B., and Ravdin, I. S. Fractures in metastatic carcinoma. American Journal of Surgery 85:282-287; 1953.

30.   Frassica, D. A. General principles of external beam radiation therapy for skeletal metastases. Clin Orthop Relat Res:S158-64; 2003.

31.   Fritz, V., Louis-Plence, P., Apparailly, F., Noel, D., Voide, R., Pillon, A., Nicolas, J. C., Muller, R., and Jorgensen, C. Micro-CT combined with bioluminescence imaging: a dynamic approach to detect early tumor-bone interaction in a tumor osteolysis murine model. Bone 40:1032-40; 2007.

32.   Fromigue, O., Lagneaux, L., and Body, J. J. Bisphosphonates induce breast cancer cell death in vitro. Journal of Bone & Mineral Research 15:2211-21; 2000.

33. Gainor, B. J., and Buchert, P. Fracture healing in metastatic bone disease. Clin Orthop Relat Res:297-302; 1983.

34. Galasko, C. S. Incidence of skeletal metastases. J Nucl Med 18:94-5; 1977.

35. Gasser, J. A., Kneissel, M., Thomsen, J. S., and Mosekilde, L. PTH and interactions with bisphosphonates. J Musculoskelet Neuronal Interact 1:53-6; 2000.

36. Goblirsch, M., Mathews, W., Lynch, C., Alaei, P., Gerbi, B. J., Mantyh, P. W., and Clohisy, D. R. Radiation treatment decreases bone cancer pain, osteolysis and tumor size. Radiation Research 161:228-34; 2004.

37. Gralow, J. R. The role of bisphosphonates as adjuvant therapy for breast cancer. Curr Oncol Rep 3:506-15; 2001.

38. Green, J. R. Antitumor effects of bisphosphonates. Cancer 97:840-7; 2003.

39. Guise, T. A., Yin, J. J., Taylor, S. D., Kumagai, Y., Dallas, M., Boyce, B. F., Yoneda, T., and Mundy, G. R. Evidence for a causal role of parathyroid hormone-related protein in the pathogenesis of human breast cancer-mediated osteolysis. J Clin Invest 98:1544-9.; 1996.

40. Hahn, M., Vogel, M., Pompesius-Kempa, M., and Delling, G. Trabecular bone pattern factor--a new parameter for simple quantification of bone microarchitecture. Bone 13:327-30; 1992.

41. Heaney, R. P. Is the paradigm shifting? Bone 33:457-65; 2003.

42. Hillner, B. E. The role of bisphosphonates in metastatic breast cancer. Semin Radiat Oncol 10:250-3; 2000.

43. Hiraga, T., Williams, P. J., Mundy, G. R., and Yoneda, T. The bisphosphonate ibandronate promotes apoptosis in MDA-MB-231 human breast cancer cells in bone metastases. Cancer Res 61:4418-24; 2001.

44. Hiraga, T., Williams, P. J., Ueda, A., Tamura, D., and Yoneda, T. Zoledronic acid inhibits visceral metastases in the 4T1/luc mouse breast cancer model. Clin Cancer Res 10:4559-67; 2004.

45. Jagdev, S. P., Coleman, R. E., Shipman, C. M., Rostami, H. A., and Croucher, P. I. The bisphosphonate, zoledronic acid, induces apoptosis of breast cancer cells: evidence for synergy with paclitaxel. British Journal of Cancer 84:1126-34; 2001.

46. Jilka, R. L., Weinstein, R. S., Bellido, T., Roberson, P., Parfitt, A. M., and Manolagas, S. C. Increased bone formation by prevention of osteoblast apoptosis with parathyroid hormone. J Clin Invest 104:439-46; 1999.

47. Keene, J. S., Sellinger, D. S., McBeath, A. A., and Engber, W. D. Metastatic breast cancer in the femur. A search for the lesion at risk of fracture. Clin Orthop Relat Res:282-8; 1986.

48. Kobayashi, S., Shimizu, T., Mehdi, R., Nawata, M., Kojima, S., Tsutsumimoto, T., Iorio, R., and Takaoka, K. Advantages of concurrent use of anabolic and antiresorptive agents over single use of these agents in increasing trabecular bone volume, connectivity, and biomechanical competence of rat vertebrae. Bone 25:703-12; 1999.

49. Kohno, N., Aogi, K., Minami, H., Nakamura, S., Asaga, T., Iino, Y., Watanabe, T., Goessl, C., Ohashi, Y., and Takashima, S. Zoledronic acid significantly reduces skeletal complications compared with placebo in Japanese women with bone metastases from breast cancer: a randomized, placebo-controlled trial. J Clin Oncol 23:3314-21; 2005.

50. Krempien, R., Huber, P. E., Harms, W., Treiber, M., Wannenmacher, M., and Krempien, B. Combination of early bisphosphonate administration and irradiation leads to improved

remineralization and restabilization of osteolytic bone metastases in an animal tumor model. Cancer 98*:*1318-24; 2003.

51. Kurth, A. A., Kim, S. Z., Sedlmeyer, I., Bauss, F., and Shea, M. Ibandronate treatment decreases the effects of tumor-associated lesions on bone density and strength in the rat. Bone 30*:*300-6; 2002.

52. Kurth, A. H., Kim, S. Z., Sedlmeyer, I., Hovy, L., and Bauss, F. Treatment with ibandronate preserves bone in experimental tumour-induced bone loss. J Bone Joint Surg Br 82*:*126-30; 2000.

53. Kurth, A. H., Wang, C., Hayes, W. C., and Shea, M. The evaluation of a rat model for the analysis of densitometric and biomechanical properties of tumor-induced osteolysis. Journal of Orthopaedic Research 19*:*200-5; 2001.

54. Legay, F., Gauron, S., Deckert, F., Gosset, G., Pfaar, U., Ravera, C., Wiegand, H., and Schran, H. Development and validation of a highly sensitive RIA for zoledronic acid, a new potent heterocyclic bisphosphonate, in human serum, plasma and urine. J Pharm Biomed Anal 30*:*897-911; 2002.

55. Levy, R. N., Sherry, H. S., and Siffert, R. S. Surgical management of metastatic disease of bone at the hip. Clin Orthop 169*:*62-9; 1982.

56. Li, X. F., Zanzonico, P., Ling, C. C., and O'Donoghue, J. Visualization of experimental lung and bone metastases in live nude mice by X-ray micro-computed tomography. Technol Cancer Res Treat 5*:*147-55; 2006.

57. Liauw, W., Segelov, E., Lih, A., Dunleavy, R., Links, M., and Ward, R. Off-trial evaluation of bisphosphonates in patients with metastatic breast cancer. BMC Cancer 5*:*89; 2005.

58. Machwate, M., Harada, S., Leu, C. T., Seedor, G., Labelle, M., Gallant, M., Hutchins, S., Lachance, N., Sawyer, N., Slipetz, D., Metters, K. M., Rodan, S. B., Young, R., and Rodan, G. A. Prostaglandin receptor EP(4) mediates the bone anabolic effects of PGE(2). Mol Pharmacol 60*:*36-41; 2001.

59. Mann, K. A., Lee, J., Arrington, S. A., Damron, T. A., and Allen, M. J. Predicting Distal Femur Bone Strength in a Murine Model of Tumor Osteolysis. Clinical Orthopaedics & Related Research in press; 2007.

60. Margulies, B. S., Schoonmaker, J. E., Strauss, J. A., Arrington, S. A., Damron, T. A., and Allen, M. J. Ewing's Sarcoma of Bone Tumor Progression in Nude Mice: Irradiation Effects on Bone Growth and Tumor Survival. Journal of Bone and Mineral Research 20 P52-53; 2005.

61. Martin, R. B., Burr, D. B., and Sharkey, N. A. Skeletal Tissue Mechanics. New York: Springer Science and Business Media, LLC; 2004.

62. Martin, T. J. Does bone resorption inhibition affect the anabolic response to parathyroid hormone? Trends Endocrinol Metab 15*:*49-50; 2004.

63. Mashiba, T., Tanizawa, T., Takano, Y., Takahashi, H. E., Mori, S., and Norimatsu, H. A histomorphometric study on effects of single and concurrent intermittent administration of human PTH (1-34) and bisphosphonate cimadronate on tibial metaphysis in ovariectomized rats. Bone 17*:*273S-278S; 1995.

64. Mirels, H. Metastatic disease in long bones. A proposed scoring system for diagnosing impending pathologic fractures. Clin Orthop Relat Res*:*256-64; 1989.

65. Miyamoto, K., Suzuki, H., Yamamoto, S., Saitoh, Y., Ochiai, E., Moritani, S., Yokogawa, K., Waki, Y., Kasugai, S., Sawanishi, H., and Yamagami, H. Prostaglandin

41

E2-mediated anabolic effect of a novel inhibitor of phosphodiesterase 4, XT-611, in the in vitro bone marrow culture. J Bone Miner Res 18:1471-7; 2003.

66. Mundy, G. Preclinical models of bone metastases. Semin Oncol 28:2-8; 2001.

67. Mundy, G. R., Yoneda, T., and Hiraga, T. Preclinical studies with zoledronic acid and other bisphosphonates: impact on the bone microenvironment. Semin Oncol 28:35-44; 2001.

68. Pan, B., To, L. B., Farrugia, A. N., Findlay, D. M., Green, J., Gronthos, S., Evdokiou, A., Lynch, K., Atkins, G. J., and Zannettino, A. C. The nitrogen-containing bisphosphonate, zoledronic acid, increases mineralisation of human bone-derived cells in vitro. Bone 34:112-23; 2004.

69. Peng, H., Sohara, Y., Moats, R. A., Nelson, M. D., Jr., Groshen, S. G., Ye, W., Reynolds, C. P., and DeClerck, Y. A. The activity of zoledronic Acid on neuroblastoma bone metastasis involves inhibition of osteoclasts and tumor cell survival and proliferation. Cancer Res 67:9346-55; 2007.

70. Peyruchaud, O., Winding, B., Pecheur, I., Serre, C. M., Delmas, P., and Clezardin, P. Early detection of bone metastases in a murine model using fluorescent human breast cancer cells: application to the use of the bisphosphonate zoledronic acid in the treatment of osteolytic lesions. Journal of Bone & Mineral Research 16:2027-34; 2001.

71. Reid, I. R., Bolland, M. J., and Grey, A. B. Is bisphosphonate-associated osteonecrosis of the jaw caused by soft tissue toxicity? Bone 41:318-20; 2007.

72. Reinholz, G. G., Getz, B., Pederson, L., Sanders, E. S., Subramaniam, M., Ingle, J. N., and Spelsberg, T. C. Bisphosphonates directly regulate cell proliferation, differentiation, and gene expression in human osteoblasts. Cancer Research 60:6001-7; 2000.

73. Rosol, T. J., Tannehill-Gregg, S. H., LeRoy, B. E., Mandl, S., and Contag, C. H. Animal models of bone metastasis. Cancer 97:748-57; 2003.

74. Santini, D., Vespasiani Gentilucci, U., Vincenzi, B., Picardi, A., Vasaturo, F., La Cesa, A., Onori, N., Scarpa, S., and Tonini, G. The antineoplastic role of bisphosphonates: from basic research to clinical evidence. Ann Oncol 14:1468-76; 2003.

75. Sato, M., Grasser, W., Endo, N., Akins, R., Simmons, H., Thompson, D. D., Golub, E., and Rodan, G. A. Bisphosphonate action. Alendronate localization in rat bone and effects on osteoclast ultrastructure. J Clin Invest 88:2095-105; 1991.

76. Senaratne, S. G., and Colston, K. W. Direct effects of bisphosphonates on breast cancer cells. Breast Cancer Res 4:18-23; 2002.

77. Senaratne, S. G., Pirianov, G., Mansi, J. L., Arnett, T. R., and Colston, K. W. Bisphosphonates induce apoptosis in human breast cancer cell lines. Br J Cancer 82:1459-68; 2000.

78. Shamir, D., Keila, S., and Weinreb, M. A selective EP4 receptor antagonist abrogates the stimulation of osteoblast recruitment from bone marrow stromal cells by prostaglandin E2 in vivo and in vitro. Bone 34:157-62; 2004.

79. Skerjanec, A., Berenson, J., Hsu, C., Major, P., Miller, W. H., Jr., Ravera, C., Schran, H., Seaman, J., and Waldmeier, F. The pharmacokinetics and pharmacodynamics of zoledronic acid in cancer patients with varying degrees of renal function. J Clin Pharmacol 43:154-62; 2003.

80. Snyder, B. D., Piazza, S., Edwards, W. T., and Hayes, W. C. Role of trabecular morphology in the etiology of age-related vertebral fractures. Calcif Tissue Int 53 Suppl 1:S14-22; 1993.

81. Thompson, E. W., Brunner, N., Torri, J., Johnson, M. D., Boulay, V., Wright, A., Lippman, M. E., Steeg, P. S., and Clarke, R. The invasive and metastatic properties of hormone-independent but hormone-responsive variants of MCF-7 human breast cancer cells. Clin Exp Metastasis 11:15-26.; 1993.

82. Tofe, A. J., Francis, M. D., and Harvey, W. J. Correlation of neoplasms with incidence and localization of skeletal metastases: An analysis of 1,355 diphosphonate bone scans. J Nucl Med 16:986-9; 1975.

83. Tong, D., Gillick, L., and Hendrickson, F. R. The palliation of symptomatic osseous metastases: final results of the Study by the Radiation Therapy Oncology Group. Cancer 50:893-9; 1982.

84. Turner, C. H., Hsieh, Y. F., Muller, R., Bouxsein, M. L., Rosen, C. J., McCrann, M. E., Donahue, L. R., and Beamer, W. G. Variation in bone biomechanical properties, microstructure, and density in BXH recombinant inbred mice. Journal of Bone & Mineral Research 16:206-13; 2001.

85. Ural, A. U., Avcu, F., Candir, M., Guden, M., and Ozcan, M. A. In vitro synergistic cytoreductive effects of zoledronic acid and radiation on breast cancer cells. Breast Cancer Res 8:R52; 2006.

86. Usui, T., Tanaka, S., Sonoda, T., Ozawa, Y., Teramura, K., Nakamura, E., Watanabe, T., and Higuchi, S. Drug disposition of incadronate, a new bisphosphonate, in rats with bone metastases. Xenobiotica 27:479-87; 1997.

87. van der Meulen, M. C., Jepsen, K. J., and Mikic, B. Understanding bone strength: size isn't everything. Bone 29:101-4; 2001.

88. von Knoch, F., Jaquiery, C., Kowalsky, M., Schaeren, S., Alabre, C., Martin, I., Rubash, H. E., and Shanbhag, A. S. Effects of bisphosphonates on proliferation and osteoblast differentiation of human bone marrow stromal cells. Biomaterials 26:6941-9; 2005.

89. Wang, C. Y., and Chang, Y. W. A model for osseous metastasis of human breast cancer established by intrafemur injection of the MDA-MB-435 cells in nude mice. Anticancer Res 17:2471-4; 1997.

90. Weber, K. L., Pathak, S., Multani, A. S., and Price, J. E. Characterization of a renal cell carcinoma cell line derived from a human bone metastasis and establishment of an experimental nude mouse model. J Urol 168:774-9; 2002.

91. Yoneda, T., Michigami, T., Yi, B., Williams, P. J., Niewolna, M., and Hiraga, T. Actions of Bisphosphonate on Bone Metastasis in Animal Models of Breast Carcinoma. Cancer Supplement 88:29792988; 2000.

92. Yoneda, T., Williams, P. J., Hiraga, T., Niewolna, M., and Nishimura, R. A bone-seeking clone exhibits different biological properties from the MDA-MB-231 parental human breast cancer cells and a brain-seeking clone in vivo and in vitro. J Bone Miner Res 16:1486-95.; 2001.

93. Yoneda, T., Williams, P. J., Hiraga, T., Niewolna, M., and Nishimura, R. A bone-seeking clone exhibits different biological properties from the MDA-MB-231 parental human breast cancer cells and a brain-seeking clone in vivo and in vitro. Journal of Bone & Mineral Research 16:1486-95; 2001.

94. Zhang, L., Endo, N., Yamamoto, N., Tanizawa, T., and Takahashi, H. E. Effects of single and concurrent intermittent administration of human PTH (1-34) and incadronate on cancellous and cortical bone of femoral neck in ovariectomized rats. Tohoku J Exp Med 186:131-41; 1998.

7. Appendices

Appendix 1: Arrington, S.A.; Schoonmaker, J.E.; Damron, T.A.; Mann, K.A.; Allen, M.J. (2006). Temporal changes in bone mass and mechanical properties in a murine model of tumor osteolysis. BONE 38, 359-367.

Appendix 2: Arrington, S.A.; Schoonmaker, J.E.; Mann, K.A.; Damron, T.A.; Sledz, T.; Willick, G.; and Allen, M.J. (2006) Zoledronic acid and PTH increase bone mass and mechanical strength following radiation therapy for osteolytic bone metastases • ABSTRACT BONE 38, Supplement 1, S43
Poster presented at the Eighth and Valedictory Workshop on Bisphosphonates: From the laboratory to the patient. Davos, Switzerland.

Appendix 3: Arrington, S.A.; Fisher, E.R.; Gasser, J.A.; Willick, G.; Allen, M.J. (December 2006) Zoledronic Acid and PTH Increase Survival and Quality of Life Following Radiation Therapy for Osteolytic Bone Metastases. Poster Presented at VI International Meeting on Cancer Induced Bone Disease. San Antonio, Texas.

Appendix 4: S. A. Arrington, B. S. Margulies, E. R. Fisher, M. J. Allen. (September 2007) *In Vitro* Effects of Zoledronic Acid Alone or in Combination with Radiation Therapy on Cells of the Metastatic Bone Environment. Poster presented at the 29th Annual American Society for Bone and Mineral Research Meeting, Honolulu, Hawaii.

Appendix 5: Arrington, S.A.; Damron, T.A; Mann, K.A.; and Allen, M.J. (2007). Concurrent Administration of Zoledronic Acid and Irradiation Leads to Improved Bone Density, Biomechanical Strength, and Microarchitecture in a Mouse Model of Tumor-Induced Osteolysis. *Journal of Surgical Oncology* (Accepted November 2007)

Appendix 6: S. A. Arrington, J. E. Schoonmaker, K. A. Mann, T. Sledz, G. Willick, T. A. Damron, and M. J. Allen. Zoledronic Acid and PTH Increase Bone Mass and Mechanical Strength Following Radiation Therapy for Osteolytic Bone Metastases. Abstract submitted to "Era of Hope" meeting, Baltimore, MA. (submitted December 2007).

Appendix 7: Curriculum Vitae